

Multiverse Understanding of Cosmological Coincidences

Raphael Bousso, Lawrence J. Hall and Yasunori Nomura

*Center for Theoretical Physics, Department of Physics
University of California, Berkeley, CA 94720-7300, U.S.A.*

and

Lawrence Berkeley National Laboratory, Berkeley, CA 94720-8162, U.S.A.

ABSTRACT: There is a deep cosmological mystery: although dependent on very different underlying physics, the timescales of structure formation, of galaxy cooling (both radiatively and against the CMB), and of vacuum domination do not differ by many orders of magnitude, but are all comparable to the present age of the universe. By scanning four landscape parameters simultaneously, we show that this quadruple coincidence is resolved. We assume only that the statistical distribution of parameter values in the multiverse grows towards certain catastrophic boundaries we identify, across which there are drastic regime changes. We find order-of-magnitude predictions for the cosmological constant, the primordial density contrast, the temperature at matter-radiation equality, the typical galaxy mass, and the age of the universe, in terms of the fine structure constant and the electron, proton and Planck masses. Our approach permits a systematic evaluation of measure proposals; with the causal patch measure, we find no runaway of the primordial density contrast and the cosmological constant to large values.

Contents

1. Introduction	2
2. A Multiverse Force and Unnatural Predictions	6
3. Parametric Dependence of Astrophysical Scales	12
3.1 Halo formation	12
3.2 Radiative cooling and galaxy formation	14
3.3 Disruption of halo formation by a positive cosmological constant	16
3.4 Compton cooling	16
4. Predicting the Virial Density and Mass of Galactic Halos	17
4.1 The catastrophic cooling boundary	17
4.2 Predictions	19
4.3 The strength of the multiverse force	20
5. Predicting the Cosmological Constant	21
5.1 Catastrophic boundary from large scale structure	21
5.2 Predictions	24
5.3 The strength of the multiverse force	26
6. Predicting the Cosmological Constant and Observer Time Scale	28
6.1 Catastrophic boundary from galaxy dispersion	29
6.2 Predictions	30
6.3 Forces with the causal patch measure	30
6.4 Forces with the causal diamond measure	32
6.5 Forces with the modified scale factor measure	33
7. Predicting the Primordial Density Contrast	34
7.1 Catastrophic boundary from Compton cooling	34
7.2 Predictions	35
7.3 Forces	36
8. Discussion	37

1. Introduction

In the evolution of the universe there are certain critical time scales that separate one era from another. The electroweak phase transition occurred at a time of order 10^{-12} sec., the QCD phase transition at order 10^{-4} sec. and the transition from radiation to matter domination at order 10^{12} sec. The time scale of inflation is very uncertain, and could be as long as a second or as short as 10^{-38} sec. Apparently the universe evolved smoothly for many decades in any given era, but between these eras, at well separated time scales, there were dramatic changes of regime.

This picture breaks down in a remarkable way during the present era. There are several time scales that originate from very different fundamental physics, and would be expected to differ by many orders of magnitude, but all have the same order of magnitude. Each of these time scales by themselves could herald a change of regime. The change from matter to vacuum domination, instigating a new era of accelerated expansion, occurs at $t_\Lambda \approx \Lambda^{-1/2}$, where $\Lambda = 8\pi G_N \rho_\Lambda$ is the cosmological constant. Another change of regime occurs at the time t_{vir} which is determined by a combination of the size of the primordial density perturbations and the temperature of matter radiation equality. At this time, density perturbations become non-linear. The universe transits out of the nearly homogeneous state it had for a number of eras and becomes clumpy. There are two possibilities for subsequent evolution. One is that the clumps or proto-galaxies cool very quickly to form galaxies, $t_{\text{cool}} \ll t_{\text{vir}}$, followed by fragmentation and star formation. In this case the change at t_{vir} is from a regime of approximate homogeneity to one of star formation. The second possibility is that $t_{\text{cool}} \gg t_{\text{vir}}$, so that there is first an era of virialized proto-galaxies, and then a much later era during which they cool. In fact, two very different processes can contribute to cooling: radiative emission and inverse Compton scattering from the background radiation, with time scales t_{rad} and t_{comp} , respectively, and the cooling time scale t_{cool} is given by the smaller of these two. Finally, once proto-galaxies have cooled, they give rise to additional time scales, including the time scale for the subsequent appearance of observers, t_{obs} , and the stellar burning time scale t_{burn} .

Other critical time scales in the past history of our universe span more than 60 orders of magnitude. Those of future phenomena, such as the decay of matter, black hole evaporation, etc., can range over thousands of orders of magnitude [1]. One might expect that the five time scales t_Λ , t_{vir} , t_{rad} , t_{comp} and t_{obs} , dependent as they are on entirely different physics, would also be well separated. Remarkably, they are all comparable,

$$t_\Lambda \sim t_{\text{vir}} \sim t_{\text{rad}} \sim t_{\text{comp}} \sim t_{\text{obs}}, \tag{1.1}$$

having an order of magnitude of 10^{10} years.¹ The picture of well separated eras breaks down during the present time, since many changes in regime are occurring simultaneously. It is hard to accept that Eq. (1.1) is purely coincidental; but it is also hard to see how it could be derived from symmetries of some underlying field theory.

If Λ varies in the multiverse, one of the coincidences of Eq. (1.1) can be explained by environmental selection. Only those universes with $t_\Lambda > t_{\text{vir}}$ have any large scale structure and can be observed [2] (see also [3]). Given that most universes have a large cosmological constant, the statistical prediction over the multiverse is $t_\Lambda \sim t_{\text{vir}}$. This result seems particularly important since it is the only known solution to the cosmological constant problem, and it predicted the discovery of nonzero vacuum energy. In fact the observed value of the cosmological constant is somewhat smaller than expected from this result [4], but it is important to note that the prediction depends on the measure used to define multiverse probability distributions. Using the causal patch measure [5], the prediction is modified to $t_\Lambda \sim t_{\text{vir}} + t_{\text{cool}} + t_{\text{obs}}$, and is more successful [6].

It is important to understand that it is legitimate in such calculations to hold all parameters but one fixed, even though many parameters can vary in the string landscape. After all, it yielded a first, nontrivial prediction that could have failed (e.g., if Λ had not been discovered). Once additional parameters are allowed to vary simultaneously, the theory has another opportunity to fail, or to succeed. A long-standing concern about the prediction for the cosmological constant is that simultaneous scanning of the virial density leads to runaway behavior favoring large values of both quantities. However, runaway behavior need not ensue if the range of new scanning parameters is constrained by additional catastrophic boundaries, and if multiverse forces point towards these boundaries.

In this paper, we study this possibility. We identify a number of possible catastrophic boundaries. We argue that under suitable assumptions about the prior distribution of parameters in the landscape, these boundaries can prevent runaway. What makes this viewpoint especially compelling is that it explains all of the coincidences in Eq. (1.1), allowing for novel cosmological predictions from environmental selection.

Outline In section 2, we review how predictions arise from multiverse probability distributions that grow towards catastrophic boundaries, across which there are significant changes in the anthropic weighting factor [7]. We stress the utility of the multiverse force, the logarithmic derivative of the distribution function, and of a set of variables chosen to be orthogonal to the catastrophic boundaries. In section 3 we review analytic

¹As a by-product of understanding these coincidences, we will find that the time scale for a main sequence star of maximal mass, t_{burn} , is constrained to be parametrically equal to these other time scales.

estimates for a number of astrophysical processes: halo virialization, halo disruption by a cosmological constant, radiative cooling, and inverse Compton cooling of proto-galaxies. Our aim is to obtain an approximate parametric dependence of astrophysical scales in our universe on parameters such as the fine structure constant, α , the electron mass, m_e , the proton mass, m_p , and Λ , which may vary in the multiverse.

In sections 4, 5, 6 and 7 we successively allow the virial density, the cosmological constant, the time scale of observers, and the Compton cooling time scale to scan. In each section, we add one more scanning parameter and one more catastrophic boundary, and we obtain one new prediction, while maintaining the previous predictions and results. At each stage, we derive the range in which multiverse forces would have to lie so that our universe is not atypical.

In section 4, we assume that the matter density at virialization scans in the multiverse. We identify a catastrophic boundary: for sufficiently small density, proto-galaxies cannot cool. Assuming a multiverse force towards small density, we find predictions for the virial density and the mass of a galaxy,

$$\rho_{\text{vir}} \sim \frac{G_{\text{N}} m_e^4 m_p^2}{\alpha^4}, \quad (1.2)$$

$$M_{\text{gal}} \sim \frac{\alpha^5}{G_{\text{N}}^2 m_e^{1/2} m_p^{5/2}}, \quad (1.3)$$

in terms of α , m_e , m_p , and the Newton constant, G_{N} . (We have omitted numerical coefficients that are displayed in the main text.) This also explains the coincidence that the timescales for radiative cooling and galactic halo virialization are comparable:

$$t_{\text{rad}} \sim t_{\text{vir}}. \quad (1.4)$$

The distance of the observed virial density from the catastrophic boundary is used to place empirical bounds on the strength of the multiverse force.

Next, in section 5, we consider scanning the cosmological constant Λ in addition to the virial density. In a certain class of measures that includes the scale factor cutoff measure proposed in Ref. [8], Λ is constrained from above by the disruption of halo formation. There is a potential runaway favoring large values of both quantities, since a larger virial density allows for a larger cosmological constant while preserving structure formation. However, for a certain range of multiverse force directions, this runaway is avoided and one predicts that typical values of the two parameters are close to the intersection of the two boundaries. This leads to a second prediction, now for the vacuum energy:

$$\rho_{\Lambda} \sim \frac{1}{G_{\text{N}} t_{\Lambda}^2} \sim \frac{G_{\text{N}} m_e^4 m_p^2}{\alpha^4}. \quad (1.5)$$

It explains, moreover, the double coincidence

$$t_\Lambda \sim t_{\text{rad}} \sim t_{\text{vir}}. \quad (1.6)$$

As in the previous section, we derive empirical constraints on the values of multiverse force components by comparing the observed ρ_Λ and ρ_{vir} to the critical values. We can compare these constraints to theoretical predictions, which depend on the measure on the multiverse, and on the prior distribution in the landscape (which is known for ρ_Λ). For the measure of [8], the empirical and theoretical limits conflict. This illustrates how our approach can be used as a systematic discriminator between measures.

In section 6, we consider a different class of measures, where the weight of observations made after t_Λ is exponentially suppressed. (This class includes the causal patch measure [5], the causal diamond measure [6], and the modified scale factor measure of [9].) In the sharp boundary approximation, catastrophe occurs unless $t_\Lambda > t_{\text{vir}} + t_{\text{obs}}$. This condition is approximately equivalent to *two* boundaries—the upper bound on the cosmological constant that appeared in the previous section, and a new boundary $t_{\text{obs}} < t_\Lambda$. Correspondingly, this class of measures allows us to scan a third parameter, t_{obs} , in addition to scanning ρ_{vir} and ρ_Λ . A wide range of multiverse forces will favor universes close to the intersection of the three catastrophic boundaries, allowing an explanation of the triple coincidence

$$t_{\text{obs}} \sim t_\Lambda \sim t_{\text{rad}} \sim t_{\text{vir}}. \quad (1.7)$$

We determine quantitative empirical constraints on force components and find that they are perfectly compatible with the prior distribution of ρ_Λ if the causal patch measure is used.

Halos that virialize in a sufficiently hot universe cool by inverse Compton scattering against the cosmic background radiation. We do not know whether this change of regime is catastrophic, but in section 7, we explore the consequences of assuming that it is. With this new boundary, we can allow a fourth parameter to scan, which we choose to be the strength of primordial density perturbations Q . In this case a further prediction follows from assuming a multiverse distribution that prefers large values of Q

$$Q \sim \frac{m_e}{m_p}. \quad (1.8)$$

Since Q and ρ_{vir} determine the temperature at equality, combining this with Eq. (1.2) yields

$$T_{\text{eq}} \sim \frac{1}{\alpha} (G_N m_e m_p)^{1/4} m_p. \quad (1.9)$$

This additional prediction, combined with Eq. (1.7), explains the quadruple coincidence

$$t_{\text{comp}} \sim t_{\text{obs}} \sim t_{\Lambda} \sim t_{\text{rad}} \sim t_{\text{vir}}. \quad (1.10)$$

In section 8, we discuss how far this program of adding more scanning parameters and catastrophic boundaries can be taken. We argue that many more predictions are possible, and we consider various ultimate solutions to runaway behavior.

2. A Multiverse Force and Unnatural Predictions

In this section, we review the approach to multiverse predictions proposed in Ref. [7]. We will also discuss the quantitative relation between the strength of a multiverse force and the proximity of typical observers to the corresponding catastrophic boundary.

A landscape of vacua, such as the string landscape, will contain scanning parameters, x , that vary between vacua [10]. We can consider any parameters that enter physical phenomena; they need not be Lagrangian parameters. The multiverse distribution

$$dN = f(x) d \ln x \quad (2.1)$$

describes the relative number of times the value x is observed, and thus its probability. In most situations, the distribution

$$f(x) = \tilde{f}(x)w(x) \quad (2.2)$$

factorizes into an a priori distribution, $\tilde{f}(x)$, of vacua in the theory landscape and an anthropic weighting factor, $w(x)$, roughly the number of observers in vacua where the parameter takes on the value x . (This number naively vanishes or diverges for all x because of eternal inflation, and a cutoff or measure is required to make it well-defined.)

Living on the edge In general, to make a prediction one needs to understand both $\tilde{f}(x)$ and $w(x)$ —the landscape, the measure, and the abundance of observers—in great detail. Under the following two conditions, however, quantitative predictions can be made even though only qualitative features of \tilde{f} and w are known:

- There are catastrophic boundaries where $w(x)$ drops sharply. Studying physics in the parameter space of x , one often discovers that there are boundaries in this space across which there is a sudden change in the physics. For example, this could be a phase transition or the stability criterion for some complex object. In the extreme limit, $w(x)$ can be represented by a theta function, so that observers are found in universes on one side of the boundary, but not in universes on the other side. This limit need not be exactly realized in practice, but it will simplify our analysis considerably.

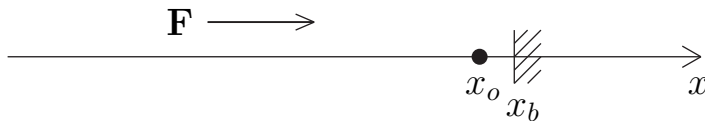


Figure 1: A strong multiverse force towards a catastrophic boundary at x_b implies that a typical observer will be located close to the boundary at x_o .

- In the region of x where observers are possible, the probability distribution, $f(x)$, increases towards the catastrophic boundary(s). Thus, most universes do not support observers.

In this situation, a typical observer would expect to measure x close to the boundary. Vacua with very different values of x either contain no observers, or are very rare in the multiverse.

The crucial point is that this quantitative prediction depends mostly on the location of the boundary, which can be calculated using the conventional law of physics. It depends only weakly on the multiverse, in that only the above qualitative assumptions on the multiverse distribution must be satisfied. This situation is illustrated in Fig. 1 for the case of a single scanning parameter with a catastrophic boundary at $x = x_b$.

The prediction $x \sim x_b$ does not follow from any symmetry of the theory; indeed it may appear coincidental. For example, it may relate two time scales or two mass scales that do not have a common origin. Since there is no symmetry reason that the observed value x_o should be close to x_b , from the conventional viewpoint the multiverse predictions appear quite unnatural.

Taking x to be the vacuum energy density, $\rho_\Lambda = \Lambda/8\pi G_N$, Fig. 1 illustrates the prediction of the cosmological constant, with $x_b \approx \rho_{\text{vir}}$. Using a logarithmic scale, the multiverse distribution indeed grows towards the boundary. This represents the cosmological constant problem. The naturalness probability, defined by $P = |\int_{x_o}^{x_b} f(x) dx / \int f(x) dx|$, is of order 10^{-120} , and from the usual symmetry viewpoint, it is extremely unnatural for ρ_Λ to take the observed value. In the multiverse picture, however, the vast majority of universes are simply irrelevant since they contain no large scale structure and thus no observers. Observing $\rho_\Lambda \sim \rho_{\text{vir}}$, therefore, is not a mystery.

Force strength The steepness of the distribution function $f(x)$ determines how close a typical observer lies to the boundary. We can refine our analysis by defining the multiverse probability force

$$F = \frac{\partial \ln f}{\partial \ln x}. \quad (2.3)$$

In this paper we will consider only power law distributions, $f(x) \propto x^p$. Then the force is simply given by the power, $F = p$. Defining x_ν to be the point such that the fraction of observers farther from the boundary than x_ν is ν , we find

$$\frac{x_\nu}{x_b} = \nu^{1/p}. \quad (2.4)$$

Thus $x_{0.5}/x_b$ is a useful measure of the typical “distance” of an observer from the boundary; it is $1/2$ for $p = 1$ and rapidly becomes smaller (larger) as p decreases (increases), since $1/p$ appears in the exponent in Eq. (2.4). For $p = 0$ the distribution is logarithmic, with equal population of all logarithmic intervals. In this case, one does not expect to find x close to x_b , so it is of no interest here.

If the force is somehow known, then we can predict not only that x should be close to x_b , but how close it should be. Roughly, one expects to measure a value of order $x_{0.5}$, and one would be mildly surprised to measure values farther from the boundary than, say, $x_{0.16}$, or closer than $x_{0.84}$.

In practice, the strength of the force is not precisely known from the theory of the landscape. We can, however, still argue that the multiverse is likely playing a role in determining the value of a parameter x if x_o is anomalously close to x_b , since such a phenomenon is extremely hard to explain in any other framework. In this circumstance, one can reverse the logic given above and derive bounds on the strength of the force; for example, if x_o is extremely close to x_b , the force is likely to be quite strong. This information can then be used to study if a certain assumption on the landscape or measure is consistent with data.

Let us make this point more precise. Given x_o and x_b , the observed and boundary values of x , Eq. (2.4) allows us to compute the force p such that a fraction ν of observers are farther from the boundary than we are:

$$p(\nu) = \frac{\ln \nu}{\ln(x_o/x_b)}. \quad (2.5)$$

For example, suppose that we are willing to reject models that would put us farther than one standard deviation from the median. Then we can infer that the multiverse force lies in the range $p(0.16)$ to $p(0.84)$. If we allow two standard deviations, the force must lie in the range $p(0.025)$ to $p(0.975)$.

As we shall see below, such empirical bounds on the multiverse force can be quite useful, for two reasons. First, there may be more than one way of obtaining a bound on the multiverse force acting on a particular parameter, allowing for a nontrivial consistency check. Second, even though we may not be able to compute the multiverse force from first principles, there may be theoretical arguments why it should satisfy a

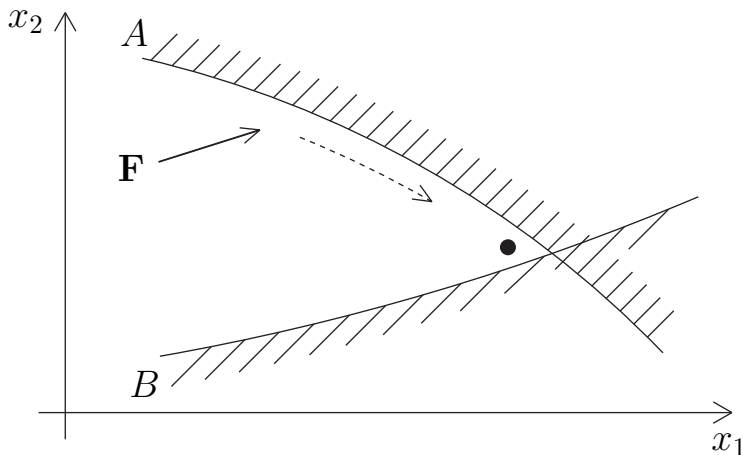


Figure 2: With two scanning parameters, (x_1, x_2) , a multiverse force towards a single catastrophic boundary, such as A , may lead to runaway behavior. The introduction of a second boundary, B , can prevent this runaway and lead to predictions for both parameters.

certain upper or lower bound. In these cases, comparison of the theoretical arguments to the empirical bounds offers a possibility of falsifying various assumptions on the properties of the landscape and the measure.

Multiple parameters Suppose that two parameters scan. Consider, for example, the catastrophic boundary labeled A in Fig. 2. In general the multiverse force is not perpendicular to the boundary, so there is now a runaway problem, as shown by the dashed arrow. This runaway behavior may be halted in several ways. A special shape of the boundary could prevent runaway, but for many boundaries this is not the case. The runaway could be prevented by $f(x)$ reaching a maximum at some point along the boundary; however, in this case this special point on the boundary results from an assumption on the form of $f(x)$ and is not predicted.

Alternatively, the runaway problem can be solved by introducing a second catastrophic boundary, as illustrated by the boundary B in Fig. 2. In this case, the boundaries define a special point by their intersection, and a multiverse force in a wide range of directions will lead to typical observers being close to this point, as shown by the dot in Fig. 2. Not only does the second boundary stop the runaway behavior, it leads to a second prediction, which will again appear coincidental and unnatural from a symmetry viewpoint. Typical observers are in universes near the “tip of the cone”, a special point in *two-dimensional* parameter space.

With n scanning parameters there could be many runaway directions. But with n boundaries of codimension one, it is possible that all the scanning parameters are

determined. With the multiverse force pointing in a generic subset of directions, the most probable observed universes will be at the tip of an n -dimensional cone, giving n predictions.

In general, these predictions will relate the scanning parameters x to fixed parameters y , which are not allowed to scan—either because they do not vary in the landscape, or because we choose to consider only a subset of the landscape. It is possible that, for the phenomena of interest, all parameters scan, and the configuration of boundaries together with our assumptions on $f(x)$ prevent any runaway and determine all the underlying parameters. In practice it may be hard to come up with such a closed, completely determined set of parameters, and the multiverse may not lead to such situations. Still, it is worth exploring how far this program of multiverse predictions can be taken.

In this paper, we consider mainly power law forces, $f(x_1, \dots, x_n) \propto \prod_{i=1}^n x_i^{p_i}$, and power law catastrophic boundaries, $\prod_{j=1}^n x_j^{b_{ij}} = \beta_i$, $i = 1, \dots, n$, which generically intersect at a critical point $(x_{1,c}, \dots, x_{n,c})$. It will be convenient to work with the logarithmic quantities

$$z_i \equiv \ln \frac{x_i}{x_{i,c}}, \quad (2.6)$$

and to use capital letters Z , P , and B , to denote the vectors and matrix constructed from z_i , p_i , and b_{ij} . Then the critical point is at $Z = 0$.

Let us define new variables $u_i \equiv b_{ij} z_j$, or

$$U \equiv BZ, \quad (2.7)$$

which measure the distances orthogonal to the n boundaries. The boundaries are defined by $u_i = 0$, $i = 1, \dots, n$. This is illustrated in the two-dimensional case in Fig. 3. Without loss of generality, we will choose signs such that $u_i > 0$ in the allowed region. The variables U are convenient to work with because the power-law form of the distribution function is preserved if one or more of the u_i are integrated out. This is not generally the case for the x_i or z_i .

With the new notation and variables, the distribution function takes the form

$$\ln f(Z) = P \cdot Z = P \cdot B^{-1}U = S \cdot U, \quad (2.8)$$

where B^{-1} denotes the inverse matrix, and we have defined

$$S \equiv (B^{-1})^T P. \quad (2.9)$$

The force vector, with components $p_i = \frac{\partial \ln f}{\partial z_i}$ in the original coordinates, has components $s_i = \frac{\partial \ln f}{\partial u_i}$ orthogonal to the boundaries. Importantly, s_i is the effective one-dimensional force on the variable u_i if all other u_j , $j \neq i$, are integrated out. (Note

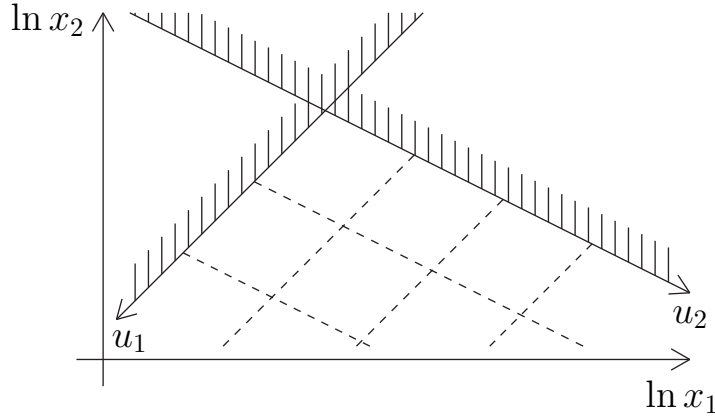


Figure 3: Given n boundary hyperplanes, it is convenient to work with new variables u_i such that the allowed region is a quadrant and the critical point is at the origin of \mathbf{R}^n . In these variables, the distance from each boundary u_i is inversely related to the corresponding multiverse force component s_i , with no mixing between components.

that the analogous statement would not hold true for the original forces and variables p_i and u_i .)

To see this, consider the one-dimensional distribution functions $\hat{f}_i(u_i) \equiv \frac{dN}{du_i}$, which can be derived from the multivariate distribution by integrating out all but one variable:

$$\hat{f}_i(u_i) \propto \int_0^\infty \prod_{j \neq i} du_j |\det B|^{-1} \exp(S \cdot U) \propto \exp(s_i u_i). \quad (2.10)$$

The one-dimensional effective force on u_i is

$$\frac{d \ln \hat{f}_i}{du_i} = s_i, \quad (2.11)$$

as claimed. With our convention that the u_i are positive in the allowed region, the s_i must all be negative to avoid runaway.

The fraction of observers farther than u_i from the boundary $u_i = 0$ is

$$\nu_i = \exp(s_i u_i). \quad (2.12)$$

If the multiverse force is known, the characteristic distances u_i can be predicted in analogy to Eq. (2.4). For example, from $\nu_i = 0.5$ one obtains the median values $u_i = s_i^{-1} \ln 0.5$. With $Z = B^{-1}U$ and Eq. (2.6), this translates into predictions for characteristic values of the original parameters x_i .

Conversely, if the multiverse force is not known, it can be constrained by demanding that the observed values not be improbably close to or far from the boundary, as in Eq. (2.5):

$$s_i(\nu) = \frac{\ln \nu}{u_{i,o}}. \quad (2.13)$$

These n constraints can be translated into constraints on the n original force components p_i , with $P = B^T S$.

The region of parameter space that allows observers – the observer region – is assumed to be open in the above analysis. However, there could be more catastrophic boundaries that make the observer region finite. If these additional boundaries are not distant from the point describing our universe, the analysis would change accordingly.

3. Parametric Dependence of Astrophysical Scales

In this section, we will discuss astrophysics in our universe. We will ask how astrophysical quantities, like the virial density and temperature, and the range of galactic masses, are related to “fundamental” parameters such α , m_e , m_p , Q , etc. Such calculations have nothing to do with the landscape or with imposing anthropic cuts; they are merely derivations of observed macroscopic phenomena from observed microphysics. A large enough computer could perform them with arbitrary accuracy, given the observed values of the input parameters.

We will not attempt a very detailed analysis. Since we will be mainly interested in the parametric dependence on the fundamental parameters, our goal is to capture the dominant physics that controls the phenomena we study. In order to compensate for analytical shortcuts and bring our simple models into precise agreement with data, we will insert suitable order one factors where necessary (for example, c_{ion} and c_{vir} below).

Note that this does not amount to putting in the answer to the central problem investigated in this paper. Our goal is to *explain* why certain combinations of fundamental parameters (namely those that appear in derived astrophysical and cosmological quantities) take on the values they do. This question becomes meaningful only in the larger setting of the multiverse, where what would otherwise be fixed input parameters like α , m_e , m_p , Q , etc., can vary. It will be considered in the following sections.

3.1 Halo formation

Complex structures, such as stars, will not form unless the virialized gas inside dark matter halos is able to cool. In our universe, there is both a maximum and a minimum characteristic halo mass for which radiative cooling is successful. (Compton cooling does not play an important role in our universe and will be considered in section 7.) In

this section we review the conditions for cooling and derive the upper and lower bounds on the halo mass.

We stress that the present section is entirely about reviewing the conventional physics of cooling in *our* universe; “fundamental” parameters like Q or m_e are taken to have the observed values. In later sections, we will consider multiverse settings in which one or more parameters scan. At that point we will make use of the parametric dependence of the expressions we derive here, in order to explain why certain parameters that scan over the multiverse are observed to take the values that they do.

We assume adiabatic, near scale-invariant, density perturbations with primordial amplitude Q . Far into the matter dominated era, a density perturbation of mass M grows linearly with the scale factor, $a(t)$, and at time t has an amplitude

$$Q(M, t) = \left(\frac{\rho(t)}{\rho_{\text{eq}}} \right)^{1/3} f(M) Q, \quad (3.1)$$

where $\rho(t)$ is the matter density and

$$\rho_{\text{eq}} = \frac{\pi^2 N_{\text{eq}} T_{\text{eq}}^4}{30} \quad (3.2)$$

is its value at the time t_{eq} when it equals the radiation density. Here, $N_{\text{eq}} \simeq 3.36$ is the number of relativistic species at the temperature of matter-radiation equality, and T_{eq} is the temperature at equality. We will consider T_{eq} the fundamental parameter that defines the time of equality.

The function $f(M)$ includes both a mild logarithmic growth for perturbations that entered the horizon before t_{eq} and complicated behavior over a lengthy transition region between radiation and matter dominated eras. For example, for $M = 10^{12} M_{\odot}$, which is close to the mass of the Milky Way, $f(M) \simeq 43$ [11].

For sufficiently small ρ_{Λ} , the perturbation on scale M goes non-linear and virializes at time defined by

$$Q(M, t_{\text{vir}}) = \delta_{\text{col}} \equiv \frac{3(12\pi)^{2/3}}{20} \simeq 1.69. \quad (3.3)$$

With Eq. (3.1), one finds

$$t_{\text{vir}} = c_{\text{vir}} \left(\frac{5 \delta_{\text{col}}^3}{\pi^3 N_{\text{eq}} f(M)^3} \frac{1}{G_{\text{N}} \bar{\rho}} \right)^{1/2}, \quad (3.4)$$

where the coefficient $c_{\text{vir}} \simeq 0.5$ is introduced to account for the effects of halo merging.² We have defined a fiducial density

$$\bar{\rho} = Q^3 T_{\text{eq}}^4, \quad (3.5)$$

²Halos grow by mergers and by accretion. Both effects contribute to the mass M in Eq. (3.3), and

which is closely related to the virial density of the halo

$$\rho_{\text{vir}} = \frac{f_\rho}{6\pi G_{\text{N}} t_{\text{vir}}^2} = \frac{\pi^2 N_{\text{eq}} f_\rho f(M)^3}{30 \delta_{\text{col}}^3 c_{\text{vir}}^2} Q^3 T_{\text{eq}}^4 \equiv \frac{\pi^2 N_{\text{eq}} f_\rho f(M)^3}{30 \delta_{\text{col}}^3 c_{\text{vir}}^2} \bar{\rho}, \quad (3.6)$$

in an approximation where the virialized halo is taken to be spherically symmetric with uniform density. Note that ρ_{vir} is a factor $f_\rho = 18\pi^2$ larger than the ambient density at t_{vir} .

3.2 Radiative cooling and galaxy formation

Galaxies form in halos only if the virialized baryonic gas can cool and condense. The temperature of the virialized halo is set by the gravitational potential energy gained by electrons and protons falling into the halo. By the virial theorem,

$$\frac{1}{2} \frac{3G_{\text{N}} M \mu}{5R_{\text{vir}}} = \frac{3}{2} T_{\text{vir}}. \quad (3.7)$$

We will take the average molecular mass μ to be $m_p/2$, so that

$$T_{\text{vir}} = \frac{G_{\text{N}} \mu}{5} \left(\frac{4\pi \rho_{\text{vir}} M^2}{3} \right)^{1/3} = \frac{\pi f(M)}{10 \delta_{\text{col}}} \left(\frac{2N_{\text{eq}} f_\rho}{45 c_{\text{vir}}^2} \right)^{1/3} G_{\text{N}} m_p M^{2/3} \bar{\rho}^{1/3}. \quad (3.8)$$

In our universe, $Q \simeq 2.0 \times 10^{-5}$ and $T_{\text{eq}} \simeq 0.82$ eV, so that a halo of mass $10^{12} M_\odot$ has $t_{\text{vir}} \simeq 3.6 \times 10^9$ years, $\rho_{\text{vir}} \simeq (1.5 \times 10^{-2} \text{ eV})^4$ and $T_{\text{vir}} \simeq 40 \text{ eV} \simeq 4.6 \times 10^5 \text{ K}$.

We can now state the conditions for cooling. First, the temperature of the halo must be large enough to give significant ionization

$$T_{\text{vir}} > c_{\text{ion}} \alpha^2 m_e, \quad (3.9)$$

where, for bremsstrahlung and hydrogen line cooling, $c_{\text{ion}} \simeq 0.05$ so that $c_{\text{ion}} \alpha^2 m_e \simeq 1.5 \times 10^4 \text{ K}$. Using Eq. (3.8), this ionization requirement leads to a minimum value of the halo mass

$$M \gtrsim M_- \equiv \left(\frac{10 \delta_{\text{col}} c_{\text{ion}}}{\pi f(M)} \right)^{3/2} \left(\frac{45 c_{\text{vir}}^2}{2N_{\text{eq}} f_\rho} \right)^{1/2} \frac{\alpha^3 m_e^{3/2}}{G_{\text{N}}^{3/2} m_p^{3/2} \bar{\rho}^{1/2}}. \quad (3.10)$$

We will comment at the end of this section on the numerical value obtained here.

they cannot be disentangled in a simple spherical collapse model. However, only major mergers lead to virialization. In a more careful analysis, the density and temperature of the virialized gas is set not at the time when the halo reaches mass M , but at the earlier time when it underwent its last major merger. Our choice of c_{vir} mimics this effect; we thank S. Leichenauer for help with selecting the value 0.5.

Second, the time scale for radiative cooling of the halo, t_{rad} , should be less than the dynamical time scale t_{dyn} [12–14], which we choose to be t_{vir} :

$$t_{\text{rad}} < t_{\text{vir}}. \quad (3.11)$$

If $T_{\text{vir}} \gtrsim 10^6$ K, the halo is fully ionized, and the radiative cooling rate is dominated by bremsstrahlung emission with a time scale at virialization of

$$t_{\text{brems}} = \frac{9}{8K} \frac{m_e^{3/2} m_p T_{\text{vir}}^{1/2}}{\alpha^3 \rho_B}, \quad (3.12)$$

where $K \simeq 3.17$, and $\rho_B = f_B \rho_{\text{vir}}$ is the baryon density in the virialized halo with $f_B \simeq 1/6$. At lower temperatures other processes are important, for example hydrogen line cooling for 10^4 K $\lesssim T \lesssim 10^6$ K, so that we write the radiative cooling rate as

$$t_{\text{rad}} = \left(\frac{9}{8K} f_{\text{rad}}(T/m_e, \alpha) \right) \frac{m_e^{3/2} m_p T_{\text{vir}}^{1/2}}{\alpha^3 \rho_B}. \quad (3.13)$$

The cooling condition of Eq. (3.11) is satisfied only by halos with mass

$$M \lesssim M_+ \equiv \left(\frac{2^7 5^{1/2} N_{\text{eq}} f_{\rho}^{5/2} K^3 f_B^3 f(M)^3}{3^8 \delta_{\text{col}}^3 c_{\text{vir}}^2 f_{\text{rad}}^3} \right) \frac{\alpha^9 \bar{\rho}}{G_{\text{N}}^3 m_e^{9/2} m_p^{9/2}}. \quad (3.14)$$

We have thus translated the ionization and cooling rate conditions into lower and upper bounds on the halo mass, Eqs. (3.10, 3.14).

In our universe, $M_- \simeq 2.9 \times 10^9 M_{\odot}$ and $M_+ \simeq 4.3 \times 10^{11} M_{\odot}$. This interval is somewhat smaller than the observed range of halo masses; in particular, it does not include our own halo, with $M \sim 10^{12} M_{\odot}$. This has a number of reasons. We have worked with 1σ overdensities to associate a typical virial density and temperature to a given mass scale. But a reasonable fraction of halos will form from, say, 2σ overdensities. This can be incorporated into Eqs. (3.10, 3.14) by substituting $f(M) \rightarrow 2f(M)$; it lowers the minimum mass by about a factor of 3 and raises the maximum mass by a factor of 8.

With this definition, the range does include the Milky Way, if only barely. This is as it should be: a halo of mass $10^{12} M_{\odot}$ is only just able to satisfy the cooling criteria [15], corresponding to the coincidence that $t_{\text{cool}} \sim t_{\text{vir}}$. The lower bound, however, is still about two orders of magnitude higher than the smallest galaxies observed in our universe, which have $M \approx 10^7 M_{\odot}$. This is because we have not included molecular cooling in our analysis. Molecular cooling can lower the cooling boundary by two orders of magnitude in our universe, but it will not have a significant effect in the neighborhood of the critical value of $\bar{\rho}$ which we will find in the following section. Hence we will ignore it here.

3.3 Disruption of halo formation by a positive cosmological constant

For definiteness, we will consider only positive values of the cosmological constant in this paper. Negative values require a different analysis, though our ultimate conclusions would remain essentially unchanged.

A cosmological constant, $\Lambda > 0$, or vacuum energy, $\rho_\Lambda = \Lambda/8\pi G_N$, will come to dominate the evolution of the scale factor when the universe reaches an age of order $t_\Lambda = (3/\Lambda)^{1/2}$, when it begins to disrupt the formation of large scale structure. At late times, it causes the universe to expand exponentially with characteristic timescale t_Λ .

A primordial overdensity which, in a flat universe with vanishing vacuum energy, would evolve into a halo with virial density ρ_{vir} will fail to evolve into a gravitationally bound object in a flat universe with [2]

$$\rho_\Lambda \gtrsim \frac{\rho_{\text{vir}}}{54}. \quad (3.15)$$

Using Eq. (3.6), one finds that the observed vacuum energy,

$$\rho_{\Lambda,o} = (2.3 \times 10^{-3} \text{ eV})^4 \quad (3.16)$$

prevents the formation of halos of mass greater than $5.4 \times 10^{14} M_\odot$ in our universe.

3.4 Compton cooling

A proto-galaxy can also cool by inverse Compton scattering of electrons from the cosmic background radiation. The cooling rate of a fully ionized plasma with temperature T against a background with temperature $T_{\text{CMB}} \ll T$ is given by

$$\frac{\dot{T}}{T} = \frac{4\sigma_T a T_{\text{CMB}}^4}{3m_e}, \quad (3.17)$$

where $\sigma_T = 8\pi\alpha^2/3m_e^2$ is the total Thompson cross section and $a = \pi^2/15$. Note that this rate does not depend on the density or temperature of the plasma. Its inverse defines the Compton cooling time scale,

$$t_{\text{comp}} = \frac{135m_e^3}{32\pi^3\alpha^2 T_{\text{CMB}}^4}, \quad (3.18)$$

which depends on cosmological time t through the CMB temperature

$$T_{\text{CMB}}(t) = \frac{5}{\pi^4 N_{\text{eq}} G_N T_{\text{eq}} t^2}. \quad (3.19)$$

Compton cooling is effective as long as this time scale, at the time of virialization, t_{vir} , is faster than the dynamical time scale of the virialized halo, which is also given by t_{vir} :

$$t_{\text{comp}}(t_{\text{vir}}) < t_{\text{vir}}. \quad (3.20)$$

Thus, Compton cooling is effective for any halos that virialize prior to the time

$$t_{\text{comp,max}} \simeq \frac{5^{1/5} 2^3}{3^{9/5} \pi^{7/5} N_{\text{eq}}^{4/5}} \frac{\alpha^{6/5}}{G_{\text{N}}^{4/5} T_{\text{eq}}^{4/5} m_e^{9/5}}. \quad (3.21)$$

In our universe, this time is approximately 0.36 Gyr.

Even before this time, Compton cooling may not be the fastest cooling process. It will be faster than radiative cooling only if $t_{\text{comp}} < t_{\text{rad}}$. However, we shall not need to investigate this condition separately in this paper, because we will be interested in situations where Compton cooling is effective for halos in which radiative cooling is on the verge of being ineffective, i.e., for halos with $t_{\text{vir}} \sim t_{\text{rad}}$.

4. Predicting the Virial Density and Mass of Galactic Halos

In this section, we will consider the consequences of allowing the characteristic virial density, $\bar{\rho}$, to scan in the multiverse. In section 4.1, we use the parametric expressions for the two cooling boundaries on the halo mass M derived in the previous section to show that there is a catastrophic lower bound on $\bar{\rho}$, where the maximum and minimum mass become equal. We assume a multiverse force that pushes $\bar{\rho}$ towards the catastrophic galaxy cooling boundary. In section 4.2, we use this qualitative assumption to obtain rough quantitative predictions of the mass of a typical halo and its virial density, in terms of α , m_e , m_p , and G_{N} . In section 4.3, we compare our result to astrophysical data. As expected, our universe is near but not exactly at the catastrophic boundary. The distance to the boundary allows us to derive empirical bounds on the strength of the multiverse force.

4.1 The catastrophic cooling boundary

Both the upper and lower bound on halo masses, Eqs. (3.10, 3.14), depend on the primordial density contrast and the temperature at equality only through the combination $\bar{\rho} = Q^3 T_{\text{eq}}^4$, which can be thought of as the characteristic virial density in the universe. We will now assume that $\bar{\rho}$ is a variable that can take on different values in the multiverse. The origin of this scanning can be via Q or T_{eq} , but we need not specify which in the analysis here. For now, we will regard Eqs. (3.10, 3.14) as functions of the scanning parameter $\bar{\rho}$, and we will phrase our assumptions in terms of the multiverse

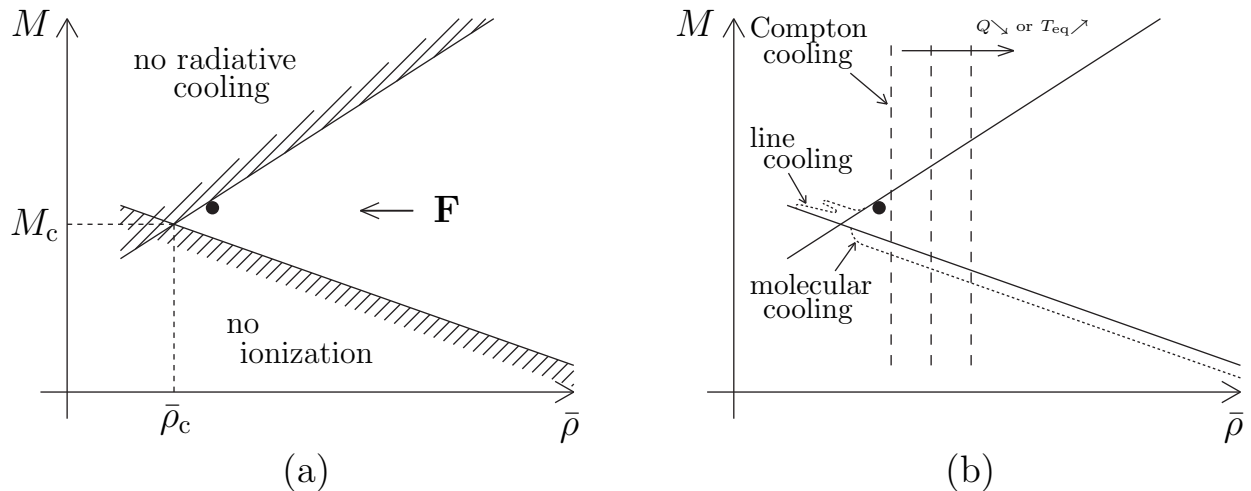


Figure 4: (a) Simplified sketch of the boundaries for ionization (lower) and radiative cooling (upper) for a halo of mass M . Our galaxy, shown by the dot, is very close to the radiative cooling boundary and has a virial density only 1 – 2 orders of magnitude larger than the minimum possible. (b) Dotted lines show modifications to the ionization and radiative cooling boundaries from molecular cooling and atomic line cooling. To the right of the dashed line, halos are able to cool by inverse Compton scattering from the background radiation.

distribution function for $\bar{\rho}$. (Later, in section 7, we will consider an additional boundary that distinguishes between Q and T_{eq} .)

These functions are sketched in Fig. 4a (with additional cooling boundaries given in Fig. 4b). Apart from the mild logarithmic factor $f(M)$, they are both simple power laws, one increasing and one decreasing with $\bar{\rho}$. They cross at the critical value

$$\bar{\rho}_c = \left(\frac{3^6 \times 5 \delta_{\text{col}}^3 c_{\text{ion}} c_{\text{vir}}^2 f_{\text{rad}}^2}{2^4 \pi f(M)^3 N_{\text{eq}} f^2 K^2 f_B^2} \right) \frac{G_{\text{N}} m_e^4 m_p^2}{\alpha^4} \simeq (0.97 \times 10^{-4} \text{ eV})^4. \quad (4.1)$$

It is important to note that M is not a scanning parameter. For any value of $\bar{\rho}$, halos with all values of M will virialize.³ We will assume, for simplicity, that observers form as long as there exists *some* range of M , no matter how small, that can cool. Thus, $\bar{\rho}_c$ represents a catastrophic boundary in $\bar{\rho}$ space. Universes with $\bar{\rho} > \bar{\rho}_c$ contain observers; universes with $\bar{\rho} < \bar{\rho}_c$ do not.

At the catastrophic boundary, only halos with critical mass

$$M_c = M_+(\bar{\rho}_c) = M_-(\bar{\rho}_c) \simeq \left(\frac{40\sqrt{5} f_\rho^{1/2} c_{\text{ion}} K f_B}{9\pi f_{\text{rad}}} \right) \frac{\alpha^5}{G_{\text{N}}^2 m_e^{1/2} m_p^{5/2}} \simeq 2.4 \times 10^{10} M_\odot \quad (4.2)$$

³This assumes that curvature and vacuum energy are negligible. We will consider nonzero vacuum energy in later sections.

and critical virial density

$$\rho_{\text{vir,c}} \simeq \left(\frac{3^5 \pi c_{\text{ion}} f_{\text{rad}}^2}{2^5 f_{\rho} K^2 f_B^2} \right) \frac{G_{\text{N}} m_e^4 m_p^2}{\alpha^4} \simeq (7.7 \times 10^{-3} \text{ eV})^4 \quad (4.3)$$

are able to cool.

Although we have been keeping track of numerical factors in the above equations, we aim only to define the position of this catastrophic boundary at the order of magnitude level. For example, there is considerable uncertainty in the numerical factor in the inequality of Eq. (3.11). The physics of cooling involves non-uniformities and shocks and, furthermore, the boundary is not completely sharp, with the statistics of merging playing an important role. Moreover, as discussed in the previous section, there is some ambiguity in how M_+ and M_- should be defined. These ambiguities arise in part because we are treating the catastrophic boundary as sharp; in a more detailed analysis, the anthropic weighting factor would change continuously over a range of values of $\bar{\rho}$. Even then, a precise estimate of the number of observers would remain a challenge.

4.2 Predictions

To obtain a prediction, we assume that the multiverse distribution $f(\bar{\rho})$ is a decreasing function. Thus, multiverse statistics favors *low* values of $\bar{\rho}$, as shown by the direction of the arrow in Fig. 4a. In this case, observers typically measure a value of $\bar{\rho}$ close to the critical value:

$$\bar{\rho} \sim \bar{\rho}_c. \quad (4.4)$$

Most universes have lower values of $\bar{\rho}$, so that no perturbations are able to cool; these universes will not be observed. Observers live only in universes with $\bar{\rho}$ sufficiently large to allow cooling. Most will find themselves near the catastrophic boundary, with $\bar{\rho}$ larger, but not much larger, than $\bar{\rho}_c$ given in Eq. (4.3).

There are a number of corollaries to this prediction. Galaxies in these universes will arise in a relatively narrow range of halo masses, controlled by the critical value M_c defined in Eq. (4.2), and ranging from a minimum halo mass of order $M_- \approx M_c (\bar{\rho}/\bar{\rho}_c)^{-1/2}$ to a maximum halo mass of order $M_+ \approx M_c (\bar{\rho}/\bar{\rho}_c)$. (The minimum mass can be lower with molecular cooling, and we have neglected logarithmic factors.) In these halos, virial densities will be larger, but not much larger, than the critical value given in Eq. (4.3); and the timescale for radiative galaxy cooling will not be much shorter than the timescale for virialization.

For the sake of clarity, let us summarize these results by restating the relevant formulas without logarithmic or order one factors. By allowing Q and/or T_{eq} to scan, and assuming a multiverse force towards small values of $\bar{\rho} = Q^3 T_{\text{eq}}^4$, we were able to

predict the observed virial density at the order of magnitude level from fundamental parameters:

$$\rho_{\text{vir}} \sim \frac{G_{\text{N}} m_e^4 m_p^2}{\alpha^4}. \quad (4.5)$$

It followed that our universe should be close to the radiative cooling boundary of Eq. (3.11):

$$t_{\text{rad}} \sim t_{\text{vir}} \sim \frac{\alpha^2}{G_{\text{N}} m_e^2 m_p}, \quad (4.6)$$

explaining one of the coincidences of Eq. (1.1); and that the galactic mass scale arises from⁴

$$M \sim \frac{\alpha^5}{G_{\text{N}}^2 m_e^{1/2} m_p^{5/2}}. \quad (4.7)$$

Another corollary is worth pointing out. The radiative cooling time scale at the critical point, Eq. (3.11), has precisely the same parametric form as the lifetime for a main sequence hydrogen burning star of maximum mass, t_{burn} . Hence, in a typical universe that is not far from the critical point, there is no freedom to choose the stellar lifetime: $t_{\text{burn}} \sim t_{\text{rad}} \sim t_{\text{vir}}$.

These predictions are successful. In our universe, $\bar{\rho}_o = Q_o^3 T_{\text{eq},o}^4 \simeq (2.4 \times 10^{-4} \text{ eV})^4$, which is only a factor of 40 larger than the critical value:

$$\bar{\rho}_o = 40 \bar{\rho}_c. \quad (4.8)$$

(We have restored order one factors.) This is remarkable since these two quantities could have been many orders of magnitude apart. It would appear even more impressive had we compared quantities of mass dimension one: $\bar{\rho}_o^{1/4} = 2.5 \bar{\rho}_c^{1/4}$. Nevertheless, $\bar{\rho}_o$ is sufficiently larger than $\bar{\rho}_c$ that in our universe galaxies with a considerable range of mass can cool radiatively. Our galaxy is near the upper end of this range, suggesting further environmental selection in our universe.

4.3 The strength of the multiverse force

The strength of the multiverse force determines how close a typical universe is to the critical point. For $\bar{\rho}$, this strength cannot be predicted from first principles with current theoretical technology. Instead, let us now reverse course and put observational constraints on the force. From Eqs. (2.5, 4.8), we conclude that the force satisfies

$$-p_{\bar{\rho}} = 0.19 \begin{smallmatrix} +0.31 \\ -0.14 \end{smallmatrix} (1\sigma) \begin{smallmatrix} +0.84 \\ -0.18 \end{smallmatrix} (2\sigma). \quad (4.9)$$

⁴Arguments that radiative cooling introduces a critical mass scale for galaxies, given by Eq. (4.2), were made in the late 1970s [12–14, 16]. Since a large range of halos on one side of the boundary can cool, however, a multiverse force and anthropic arguments are needed to explain why observed galaxies are so close to this critical value.

Note that the force discussed here is the effective force obtained after integrating out parameters other than $\bar{\rho}$ [7], such as the cosmological constant. In the following sections we will consider such parameters, and we will be able to determine under which conditions a force in the above range can arise. We will see that this places interesting constraints on the multiverse distribution function, and in particular, on the measure for regulating the infinities of eternal inflation.

5. Predicting the Cosmological Constant

In this section, we will allow a second parameter to scan: the cosmological constant or vacuum energy, ρ_Λ .⁵ To avoid runaway, we need a second boundary. One way to obtain such a boundary is to require, as in the previous section, that galaxies form [2]. This condition is clearly necessary; whether it is the most important constraint on ρ_Λ depends on the choice of measure. As shown in Ref. [9], the version of the scale factor measure formulated in Ref. [8] leads to this constraint.

We will be able to explain the coincidence $t_{\text{vir}} \sim t_\Lambda$ in this way. We will also be able to use observed values of $\bar{\rho}$ and ρ_Λ to constrain the two-dimensional multiverse forces on these parameters. We will find, however, that these empirical constraints lead to tension with theoretical expectations. This, therefore, disfavors the measure we consider here.

In the next section we will consider a different class of measures which will be more successful, and also more powerful in that they constrain an additional scanning parameter.

5.1 Catastrophic boundary from large scale structure

The role of the measure In theories with at least one long-lived metastable vacuum with positive cosmological constant, a finite false vacuum region can evolve into an infinite four-volume containing infinitely many bubbles of other vacua. Each bubble is an infinite open universe; if it contains any observers, no matter how sparse, it will contain infinitely many. These infinities must be regulated if we are to say that some outcomes of observations are typical and others unlikely. This is the measure problem of eternal inflation.

We will consider four measure proposals that are reasonably well-defined and do not suffer from known catastrophic problems.⁶ The first and second are the causal patch [5] (CP) and causal diamond (CD) [6] cutoffs; the third and fourth are versions

⁵For definiteness, we will consider only positive values of the cosmological constant, although it is not difficult to extend our analysis to negative values.

⁶The measures used in the older literature on environmental selection of the cosmological constant,

of the scale factor cutoff, which we will refer to as SF1 [8] and SF2 [9]. We will not review these measures here in detail, but focus instead on their implications for the analysis of the cosmological constant problem. The measures differ in important ways: they lead not only to different catastrophic boundaries, but also to different multiverse forces on the cosmological constant and virial density.

Both measures are based on a geometric cutoff: one computes the expected number of observations made in some finite spacetime region. They differ in how that region is defined. The causal patch measure (CP) restricts to the causal past of the future endpoint of a geodesic in the spacetime. In long-lived metastable vacua with positive cosmological constant, this definition reduces to counting observations that take place within the cosmological (de Sitter) event horizon surrounding the geodesic. This has two important consequences. First, observations made after vacuum domination ($t_{\text{obs}} > t_{\Lambda}$) contribute negligibly; they are exponentially suppressed by the accelerated expansion that empties the horizon region of matter. This leads to a catastrophic boundary $\Lambda \lesssim t_{\text{obs}}^{-2}$.⁷ Secondly, at all times before vacuum domination ($t < t_{\Lambda}$), the total matter mass inside the causal patch scales as $\Lambda^{-1/2}$. For smaller Λ , more matter is included, which mitigates the landscape force towards large values of Λ .

The causal diamond (CD) cutoff further restricts the surviving spacetime region. A point is included only if it lies both in the causal patch and in the causal future of the intersection of the generating geodesic with the reheating hypersurface. This leads to the same catastrophic boundary, $\Lambda \lesssim t_{\text{obs}}^{-2}$. However, before t_{Λ} , the comoving volume of the diamond is controlled by the future light-cone. Thus it is independent of Λ and grows linearly with time. This favors later observers.

As shown in Ref. [9], the scale factor cutoff (SF1) can be defined as a small neighborhood, of fixed physical volume, of a geodesic in the multiverse. (The formulation of

such as observers-per-baryon, fail catastrophically in eternally inflating universes driven by false vacua [17, 18], so they will not be considered here. For other examples of catastrophic problems, see, e.g., Ref. [19].

⁷This boundary is stronger than the catastrophic boundary coming from the disruption of galaxy formation. Of course, nothing prevents the formation of observers in a universe where suitable galaxies form. However, such observers are not counted if the galaxies are not contained in the cutoff region. The existence of such a boundary, coming entirely from the measure, may seem counter-intuitive; indeed, it is among the most interesting lessons learned from recent studies of the measure problem [6]. In eternal inflation, no conventional anthropic boundary is well-defined without a measure. For example, with $\Lambda \gg t_{\text{vir}}^{-2}$, there is still a tiny amplitude for the formation of galaxies from unusually strong density perturbations, so there will be infinitely many observers no matter whether Λ is above or below the Weinberg bound. To make a meaningful comparison, we need to pick a measure. The measures usually considered are geometric cutoffs that necessarily depend on quantities that affect the geometry, such as Λ . It should not surprise us, then, that they can introduce catastrophic boundaries on observable parameters.

the scale factor measure given in Ref. [8] is not completely equivalent but shares the following properties [9]⁸ relevant for our analysis.) Like in the CD measure, and unlike CP, the size of the SF1 cutoff region is independent of Λ before the time t_Λ . Because the geodesic is likely to become trapped in a collapsed region, and one is including only its immediate neighborhood, the expansion of the universe after t_{vir} does not reduce the number of observers contained in the cutoff region. This leads to two important differences from both CD and CP. First, there is no suppression for $t_{\text{obs}} > t_\Lambda$, so the only relevant catastrophic boundary is the Weinberg bound, $\Lambda \lesssim t_{\text{vir}}^{-2}$. And secondly, in SF1 the number of observers is proportional to their physical density near the geodesic; this favors larger virial density.

SF2 is a hybrid of SF1 and CD. This measure has only been tentatively formulated [9], but we include it here because we are mainly interested in the consequences of a measure with the following properties: like in the CD measure, the catastrophic boundary is $\Lambda \lesssim t_{\text{obs}}^{-2}$, and the spatial size of the cutoff region is Λ -independent before t_Λ . The number of observers is proportional to the average density of matter in the universe at the time when observations are made. This is similar to SF1, except that for SF1 the relevant density is set at an earlier time, when the first collapsed structures form.

In this section, we begin by considering the catastrophic boundary relevant to SF1: the disruption of the formation of galactic halos. In section 6, we will consider the catastrophic boundary relevant to CP, CD, and SF2: the exponential dilution of the number density of galaxies. For each case, we will obtain predictions for scanning parameters and empirical constraints on multiverse forces. We will discuss whether these constraints are compatible with theoretical expectations, which also depend on the measure.

The boundary In a given universe, the cosmological constant disrupts the formation of halos above a certain mass, because the logarithmic factor $f(M)$ in Eq. (3.6) will enter into the condition of Eq. (3.15). It is possible that there is a minimum galaxy mass necessary for the formation of observers. As in the previous section, however, we will work with the conservative assumption that any galaxies will do. Thus, a catastrophic boundary for the cosmological constant is reached only when ρ_Λ is so large as to disrupt the formation of the smallest halos that can cool. By Eq. (3.15), this corresponds to the condition

$$\rho_{\Lambda, \text{max}}(\bar{\rho}) = \frac{\rho_{\text{vir}}(M_-(\bar{\rho}))}{54}, \quad (5.1)$$

⁸This was not originally recognized in Ref. [8], who concluded that the properties of their formulation were similar to those ascribed here to SF2.

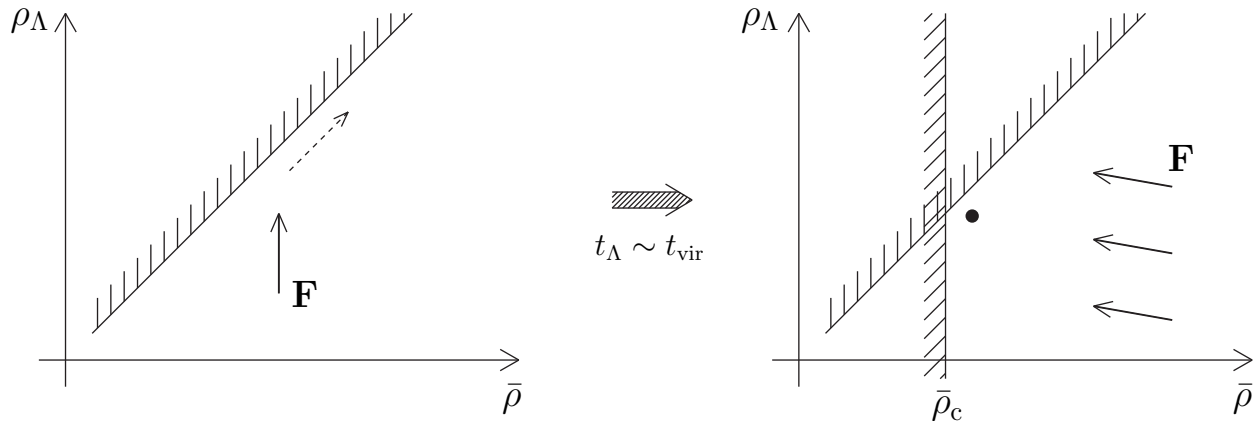


Figure 5: When both ρ_Λ and the virial density $\bar{\rho}$ scan, the resulting behavior depends on the direction of the multiverse force and on the boundaries. On the left, a multiverse force with only a ρ_Λ component leads to runaway behavior along the virialization boundary, as shown by the dashed arrow. On the right, a component of the force in the direction of $\bar{\rho}$ is added, as well as the boundary from galactic radiative cooling. Typical universes lie at the tip of the cone, indicated by the dot. Strong forces would locate the dot within a factor of two of each boundary. But the forces may be mild, placing the dot one to two orders of magnitude from the boundaries, as observed in our universe. With an accuracy that depends on the strength of the force, multiverse predictions result for both ρ_Λ and $\bar{\rho}$ in terms of the fundamental parameters that determine the location of the boundaries.

where $\rho_{\text{vir}}(M_-)$ and $M_-(\bar{\rho})$ are given in Eqs. (3.6) and (3.10).

Up to logarithmic corrections from $f(M_-)$, this catastrophic boundary corresponds to a line of slope 1 in the $(\bar{\rho}, \rho_\Lambda)$ plane shown in Fig. 5. Of course, the analysis in the following subsection would apply to any measure in which this line is the relevant catastrophic boundary.

5.2 Predictions

We have already assumed a force towards large vacuum energy ρ_Λ , and we have established two catastrophic boundaries, Eqs. (4.1, 5.1). These boundaries intersect at the critical point

$$(\bar{\rho}, \rho_\Lambda) = (\bar{\rho}_c, \rho_{\Lambda,c}), \quad (5.2)$$

where

$$\rho_{\Lambda,c} \equiv \rho_{\Lambda,\text{max}}(\bar{\rho}_c) = \left(\frac{3^2 \pi c_{\text{ion}} f_{\text{rad}}^2}{2^6 f_\rho K^2 f_B^2} \right) \frac{G_N m_e^4 m_p^2}{\alpha^4} \simeq (2.8 \times 10^{-3} \text{ eV})^4. \quad (5.3)$$

Here, we have used the expression for $\rho_{\text{vir},c}$ given in Eq. (4.3).

Whether these critical values become predictions depends on the sign and magnitude of the force component in the $\bar{\rho}$ direction, $p_{\bar{\rho}} \equiv \partial \ln f / \partial \ln \bar{\rho}$. (Note that this is not the same as the force on $\bar{\rho}$ considered in the last section, which was understood to result from integrating out all other scanning parameters, such as Λ .)

The left panel of Fig. 5 shows the runaway problem that would arise in the absence of a sufficiently strong force toward small $\bar{\rho}$, i.e., if $p_{\bar{\rho}} > -p_{\Lambda}$. The total force points to the structure formation boundary, but once this boundary is reached, the component tangential to the boundary goes in the positive ρ_{Λ} and $\bar{\rho}$ directions, giving the runaway behavior indicated by the dashed line. The cosmological constant problem is not solved in this case. Moreover, the prediction for $\bar{\rho}$ in the previous section would also be lost, since the effective force on $\bar{\rho}$, after integrating out Λ , would point towards large values.

Let us assume, therefore, that $p_{\bar{\rho}} < -p_{\Lambda}$, i.e., the force towards small $\bar{\rho}$ is strong enough to overwhelm the force towards large ρ_{Λ} once the catastrophic structure formation boundary is reached. In this case, as shown in the right panel of Fig. 5, the force selects the tip of the cone formed by the two boundaries as the most likely universe, and we obtain two predictions:

$$\begin{aligned}\bar{\rho} &\sim \bar{\rho}_c \simeq (0.97 \times 10^{-4} \text{ eV})^4, \\ \rho_{\Lambda} &\sim \rho_{\Lambda,c} \simeq (2.8 \times 10^{-3} \text{ eV})^4.\end{aligned}\tag{5.4}$$

Recall that $\bar{\rho}_c$ and $\rho_{\text{vir},c}$, given in Eqs. (4.1) and (4.3), have the same parametric dependence on fundamental parameters and differ only through numerical factors. Neglecting such factors, we are able to relate both $\bar{\rho}$ and ρ_{Λ} to fundamental parameters as

$$\bar{\rho} \sim \rho_{\Lambda} \sim \frac{G_{\text{N}} m_e^4 m_p^2}{\alpha^4}.\tag{5.5}$$

As a corollary, we are able to explain the double coincidence

$$t_{\Lambda} \sim t_{\text{rad}} \sim t_{\text{vir}} \sim \frac{\alpha^2}{G_{\text{N}} m_e^2 m_p}.\tag{5.6}$$

Thus, we predict that most observers will find themselves in a universe with $\bar{\rho}$ larger, but not much larger, than $\bar{\rho}_c$, and with ρ_{Λ} comparable to $\bar{\rho}_{\text{vir},c}/54$. (Note that ρ_{Λ} could be smaller or larger than this critical value, because the catastrophic boundary is not a line of constant ρ_{Λ} . However, it should not differ very much from the critical value.)

The first prediction in Eq. (5.4) reproduces our successful result in section 4.2, and it yields the same corollaries: predictions for the characteristic mass, virial density, and cooling timescale of galactic halos. The second prediction addresses the cosmological

constant problem. This prediction, too, is successful: the observed vacuum energy, $\rho_{\Lambda,o} = (2.3 \times 10^{-3} \text{ eV})^4$, is only a factor 2.1 smaller than the critical value.

This might suggest that the force on the cosmological constant must be strong. But this is not the case. To gauge the multiverse forces, we must compute the distances orthogonal to the catastrophic boundaries. We shall now see that this constrains the force on the cosmological constant to be quite weak.

5.3 The strength of the multiverse force

We now have a two-dimensional parameter space, with variables

$$z_1 = \ln \frac{\bar{\rho}}{\bar{\rho}_c}, \quad (5.7)$$

$$z_2 = \ln \frac{\rho_\Lambda}{\rho_{\Lambda,c}}. \quad (5.8)$$

By Eq. (2.7), the matrix

$$B = \begin{pmatrix} 1 & 0 \\ 1 & -1 \end{pmatrix} \quad (5.9)$$

defines two new parameters

$$u_1 = \ln \frac{\bar{\rho}}{\bar{\rho}_c}, \quad (5.10)$$

$$u_2 = \ln \frac{\rho_{\Lambda,\max}(\bar{\rho})}{\rho_\Lambda}, \quad (5.11)$$

that are orthogonal to catastrophic boundaries at $u_1 = 0$ and $u_2 = 0$, where $\rho_{\Lambda,\max}$ is given in Eq. (5.1). (We have used that $\rho_{\Lambda,\max}$ is proportional to $\bar{\rho}$, up to a logarithmic term which we neglect.)

By Eq. (2.9), $(B^{-1})^T$ defines associated force components S , with

$$s_1 = p_{\bar{\rho}} + p_\Lambda, \quad (5.12)$$

$$s_2 = -p_\Lambda, \quad (5.13)$$

acting on the parameters U . The absence of a runaway problem corresponds to the condition $s_i < 0$, $i = 1, 2$, which agrees with the force conditions we identified in section 5.2 above.

The observed values in our universe are

$$u_{1,o} \simeq \ln 40 \simeq 3.7, \quad (5.14)$$

$$u_{2,o} \simeq \ln 139 \simeq 4.9. \quad (5.15)$$

The second line is the statement that the cosmological constant in our universe is more than a hundred times smaller than necessary for large scale structure formation. By demanding that these observed values are within one or two standard deviations from the median, we obtain from Eq. (2.13) that

$$p_{\bar{\rho}} + p_{\Lambda} = - \left[0.19 \begin{smallmatrix} +0.31 \\ -0.14 \end{smallmatrix} (1\sigma) \begin{smallmatrix} +0.84 \\ -0.18 \end{smallmatrix} (2\sigma) \right], \quad (5.16)$$

$$-p_{\Lambda} = - \left[0.141 \begin{smallmatrix} +0.233 \\ -0.106 \end{smallmatrix} (1\sigma) \begin{smallmatrix} +0.626 \\ -0.136 \end{smallmatrix} (2\sigma) \right]. \quad (5.17)$$

Note that the right hand side of Eq. (5.16) is the same as the constraint on the force $p_{\bar{\rho}}$ derived in the one-dimensional setting of Eq. (4.9). This is as it should be. The left hand side looks different, but this is a notational problem: in the previous section, $p_{\bar{\rho}}$ was understood to include all contributions from integrating out other parameters and boundaries. Here, however, the contribution from p_{Λ} was excluded in the definition of $p_{\bar{\rho}}$. It thus appears explicitly in Eq. (5.16).

How do these bounds compare to theoretical expectations? Because 0 is not a special point in the spectrum of the cosmological constant, one can treat the statistical distribution of ρ_{Λ} as flat in a small neighborhood of 0 (and only an extremely small neighborhood is of interest anthropically):

$$\frac{d\tilde{f}}{d\rho_{\Lambda}} = \text{const}, \quad (5.18)$$

at least after smoothing over intervals much smaller than the observed value. Thus, the simplest theoretical expectation is a force of unit strength towards large values of Λ :

$$\tilde{p}_{\Lambda} \equiv \frac{\partial \ln \tilde{f}}{\partial \ln \rho_{\Lambda}} = 1. \quad (5.19)$$

This result, however, is modified (in different ways) by all of the measures we consider here.

The catastrophic boundary we have used—the Weinberg bound on the formation of galactic halos—arises from the scale factor measure as formulated by De Simone *et al.* [8, 9]. Correspondingly, we should here consider the implications of this particular measure for the strength of F_{Λ} . We will compare this theoretical expectation to our empirical constraint, Eq. (5.17).

Let \hat{n}_{obs} be the number density of observers per physical volume at the time $t_{\text{vir}} + t_{\text{obs}}$ when observations are made in a given bubble universe. As shown in Ref. [9], the scale factor measure weights observers by the physical number density these observers would have had at the time when the first structures formed that would eventually be

incorporated into their halo. This weight is approximately

$$w_{\text{SF1}} \propto \left(\frac{\hat{n}_{\text{obs}}}{\rho_{\text{obs}}} \right) \rho_{\text{vir}}, \quad (5.20)$$

where ρ_{obs} is the matter density at the time $t_{\text{vir}} + t_{\text{obs}}$. The first factor is the number of observers per unit mass. In our sharp-boundary approximation, this factor is constant and nonzero on the anthropic side of the catastrophic boundaries in the $(\bar{\rho}, \rho_{\Lambda})$ plane. Beyond the cooling and structure boundaries, it vanishes.

The second factor, up to numerical coefficients, agrees with $\bar{\rho}$, so the weight w_{SF1} contributes a single power of $\bar{\rho}$ to the distribution function f . Thus, the force on the anthropic side receives a contribution

$$(\Delta p_{\bar{\rho}}, \Delta p_{\Lambda})_{\text{SF1}} = (1, 0) \quad (5.21)$$

from the measure. Therefore, the total force is $(p_{\bar{\rho}}, p_{\Lambda}) = (1 + \tilde{p}_{\bar{\rho}}, 1)$, where $\tilde{p}_{\bar{\rho}} \equiv \partial \ln \tilde{f} / \partial \ln \bar{\rho}$ is the unknown contribution from the distribution of $\bar{\rho}$ among landscape vacua. For the linear combinations constrained in Eqs. (5.16, 5.17), we find

$$(p_{\bar{\rho}} + p_{\Lambda}, p_{\Lambda}) = (2 + \tilde{p}_{\bar{\rho}}, 1). \quad (5.22)$$

The first constraint can be satisfied by assuming that the unknown prior landscape force, $\tilde{p}_{\bar{\rho}}$, lies between -2 and -3 . While this may seem like an implausibly strong force towards small virial density—an inverse power law of mass dimension -8 to -12 —we cannot rule out that it may be realized in the string landscape.

The second constraint, however, on the force on Λ , is definitely incompatible with the theoretical expectation at the 2σ level. (It would be compatible at the 3σ level.) Thus, with the scale factor measure in the formulation of De Simone *et al.* [8], multiverse forces cannot simultaneously explain ρ_{vir} and ρ_{Λ} without additional assumptions.

6. Predicting the Cosmological Constant and Observer Time Scale

In this section, we will again consider the case of scanning both the cosmological constant ρ_{Λ} and the virial density parameter $\bar{\rho}$, but using a different measure for regulating the divergences of the eternally inflating multiverse. In the previous section we used the scale factor measure in the formulation of Ref. [8] (SF1). We will now explore the implications of the causal patch (CP) [5], causal diamond (CD) [6], and modified scale factor (SF2) [9] measures. We will find important differences to the previous section, and subtle differences among the three measures we now consider:

- All three measures yield the same set of three catastrophic boundaries, in the three-dimensional parameter space $(\bar{\rho}, \rho_\Lambda, t_{\text{obs}})$. The first two boundaries are the same as for the SF1 measure; the boundary on t_{obs} is new.
- Because of the appearance of t_{obs} , we will allow three parameters to vary in this section: $\bar{\rho}$, ρ_Λ , and t_{obs} .
- The three measures make different contributions to the multiverse force vector. We will find observational constraints on the corresponding multiverse forces that are in excellent (CP, CD) or reasonable (SF2) agreement with theoretical expectations.

6.1 Catastrophic boundary from galaxy dispersion

All three measures considered in this section exponentially suppress the weight of observations that take place after the cosmological constant dominates, like $\exp(-3t/t_\Lambda)$. There is some ambiguity about which critical value to pick in the sharp-boundary approximation. We will use $t_\Lambda \equiv (8\pi G_N \rho_\Lambda/3)^{-1/2}$, but our results do not depend sensitively on small modifications of this choice.

Thus, in the sharp boundary approximation, we require

$$t_{\text{vir}} + t_{\text{obs}} < t_\Lambda, \quad (6.1)$$

as a necessary condition for the existence of observers. Here, we define t_{obs} as the time delay between the formation of a galactic halo at time t_{vir} and the time when the halo hosts observers. (We neglect the cooling time scale, which must not exceed t_{vir} in any case.) The delay t_{obs} includes the time needed for the formation of a solar system and Darwinian evolution, or whatever other forms the development of life in gravitationally collapsed structure may take. We have no idea how to relate t_{obs} to fundamental particle physics or cosmological parameters, but we will assume that it depends on sufficiently many parameters, sufficiently sensitively, that we can treat it as scanning independently of the other four parameters we are varying in this paper ($\bar{\rho}$, t_{rad} , ρ_Λ , and Q).⁹

In the presence of power law forces on $\bar{\rho}$ and t_{obs} , we make a negligible error if we write Eq. (6.1) as two independent catastrophic boundaries:

$$t_{\text{obs}} < t_\Lambda, \quad (6.2)$$

$$t_{\text{vir}} < t_\Lambda. \quad (6.3)$$

⁹Note that our treatment of t_{obs} is not very different from t_Λ . Neither quantity can be simply computed from “fundamental” parameters of our vacuum, but both are expected to scan in the multiverse. We predict both quantities by correlating them with other scales.

The existence of galaxies, of course, remains a necessary condition for observers, and it yields a bound tighter than Eq. (6.3): from Eq. (5.1) we find

$$t_{\text{vir}} < \frac{\pi}{3^{3/2}} t_{\Lambda} \simeq 0.60 t_{\Lambda}. \quad (6.4)$$

Thus, we will use Eq. (6.2) as the new catastrophic boundary for the new parameter t_{obs} . We will continue to treat $\rho_{\text{vir}}/54$, from Eq. (5.1), as a catastrophic upper bound on ρ_{Λ} , and $\bar{\rho}_c$, given in Eq. (4.1), as a catastrophic lower bound on $\bar{\rho}$.

6.2 Predictions

The three boundaries we have established intersect at the critical point

$$(\bar{\rho}, \rho_{\Lambda}, t_{\text{obs}}) = (\bar{\rho}_c, \rho_{\Lambda,c}, t_{\text{obs},c}), \quad (6.5)$$

where

$$t_{\text{obs},c} = t_{\Lambda}(\rho_{\Lambda,c}) = \frac{2^{3/2} f_{\rho}^{1/2} K f_B}{3^{1/2} \pi c_{\text{ion}}^{1/2} f_{\text{rad}}} \frac{\alpha^2}{G_{\text{N}} m_e^2 m_p} \simeq 11.0 \text{ Gyr}. \quad (6.6)$$

Supposing that the three-dimensional multiverse force points towards this critical point, we predict that observed values of these parameters should be within one or two orders of magnitude of the critical values. The predictions for $\bar{\rho}$ and ρ_{Λ} are the same as in the previous sections. The new prediction for t_{obs} is that it should not differ much from $t_{\text{obs},c}$, given above:

$$t_{\text{obs}} \sim t_{\text{obs},c}. \quad (6.7)$$

The observed value is

$$t_{\text{obs},o} = 10.1 \text{ Gyr}, \quad (6.8)$$

so this third basic prediction is also successful.

We have now explained the triple coincidence

$$t_{\text{obs}} \sim t_{\Lambda} \sim t_{\text{rad}} \sim t_{\text{vir}} \sim \frac{\alpha^2}{G_{\text{N}} m_e^2 m_p}. \quad (6.9)$$

Next, we will determine under which conditions the multiverse force points towards the critical point, and we will establish empirical constraints on the the three force components.

6.3 Forces with the causal patch measure

In addition to the variables z_1 and z_2 defined in section 5.3, we now have the third scanning parameter

$$z_3 = \ln \frac{t_{\text{obs}}}{t_{\text{obs},c}}. \quad (6.10)$$

The matrix

$$B = \begin{pmatrix} 1 & 0 & 0 \\ 1 & -1 & 0 \\ 0 & -1 & -2 \end{pmatrix} \quad (6.11)$$

defines the boundary-orthogonal parameter

$$u_3 = \ln \left(\frac{3}{8\pi G_N} \frac{1}{\rho_\Lambda t_{\text{obs}}^2} \right). \quad (6.12)$$

By Eq. (2.9), $(B^{-1})^T$ defines a boundary-orthogonal force vector S , with

$$s_1 = p_{\bar{\rho}} + p_\Lambda - \frac{1}{2} p_{\text{obs}}, \quad (6.13)$$

$$s_2 = -p_\Lambda + \frac{1}{2} p_{\text{obs}}, \quad (6.14)$$

$$s_3 = -\frac{1}{2} p_{\text{obs}}, \quad (6.15)$$

where $p_{\text{obs}} = \partial \ln f / \partial \ln t_{\text{obs}}$. The absence of a runaway problem, i.e., the condition that the multiverse force points towards the critical point, is that all $s_i < 0$. In particular, we learn that it is necessary to assume a statistical preference for a large time scale for the development of observers in gravitationally bound regions. This assumption seems plausible, given the complex processes that are likely to be involved. Since p_Λ appears only in the combination $p_\Lambda - \frac{1}{2} p_{\text{obs}}$, this preference acts counter to the multiverse force towards large cosmological constant. This, too, is intuitively plausible: there are fewer vacua with smaller cosmological constant, but on average they contain more observers.

From the observed values in our universe we find

$$u_{1,o} \simeq \ln 40 \simeq 3.7, \quad (6.16)$$

$$u_{2,o} \simeq \ln 139 \simeq 4.9, \quad (6.17)$$

$$u_{3,o} \simeq \ln 2.5 \simeq 0.92. \quad (6.18)$$

The fact that u_3 is of order unity is closely related to the coincidence problem: we live in the unique era when vacuum and matter energy densities are comparable. By demanding that these observed values are within one or two standard deviations from the median, we obtain from Eq. (2.13) that

$$p_{\bar{\rho}} + p_\Lambda - \frac{1}{2} p_{\text{obs}} = - \left[0.19 \begin{matrix} +0.31 \\ -0.14 \end{matrix} (1\sigma) \begin{matrix} +0.84 \\ -0.18 \end{matrix} (2\sigma) \right], \quad (6.19)$$

$$-p_\Lambda + \frac{1}{2} p_{\text{obs}} = - \left[0.141 \begin{matrix} +0.233 \\ -0.106 \end{matrix} (1\sigma) \begin{matrix} +0.626 \\ -0.136 \end{matrix} (2\sigma) \right], \quad (6.20)$$

$$-\frac{1}{2} p_{\text{obs}} = - \left[0.76 \begin{matrix} +1.25 \\ -0.57 \end{matrix} (1\sigma) \begin{matrix} +3.37 \\ -0.73 \end{matrix} (2\sigma) \right]. \quad (6.21)$$

The first two constraints are identical to those found in the previous section, except that the contribution to the multiverse force from p_{obs} is now made explicit on the left hand side.

How do these bounds compare to theoretical expectations? As reviewed in the previous section, the statistical distribution of Λ in the landscape is flat, giving a prior force $\tilde{p}_\Lambda = 1$ towards large values. As discussed at the beginning of this section, the three measures differ in the spatial size of the cutoff region. On the anthropic side of the catastrophic boundary, the number of observers included depends differently on t_{obs} and ρ_Λ for each measure. This means that the measures make different contributions to the multiverse force vector. We will discuss each measure in turn, beginning with the CP measure.

The CP measure contributes a factor $\rho_\Lambda^{-1/2}$ [6]:

$$w_{\text{CP}} = \left(\frac{\hat{n}_{\text{obs}}}{\rho_{\text{obs}}} \right) \rho_\Lambda^{-1/2}, \quad (6.22)$$

where the first factor, the density of observers per unit mass, is again approximated as constant on the anthropic side of the catastrophic boundaries and zero beyond. Thus, the CP measure makes no contribution to the forces on $\bar{\rho}$ and t_{obs} , and we find:

$$(\Delta p_{\bar{\rho}}, \Delta p_\Lambda, \Delta p_{\text{obs}})_{\text{CP}} = (0, -\frac{1}{2}, 0). \quad (6.23)$$

The CP measure, therefore, leads to a reduced force on the cosmological constant:

$$p_\Lambda = \frac{1}{2}. \quad (6.24)$$

In Eq. (6.20), p_Λ and the force towards large observer time scale appear with opposite sign, reducing the magnitude of the left hand side further. This should be compared to the analogous equation Eq. (5.17) for the SF1 measure, which contained only $p_\Lambda = 1$, and so could not be satisfied at the 2σ level. By contrast, the above three empirical constraints are all compatible with Eq. (6.24) at the 1σ level. Possible values for $(p_{\bar{\rho}}, p_{\text{obs}})$ include $(-\frac{1}{2}, \frac{1}{2})$ and $(-\frac{1}{4}, \frac{3}{4})$.

6.4 Forces with the causal diamond measure

How would this discussion be modified if we used the CD measure? The catastrophic boundaries remain unchanged, preserving both the general prediction that we should find ourselves near the triple critical point $(\bar{\rho}_c, \rho_{\Lambda,c}, t_{\text{obs},c})$, and the empirical constraints given in Eqs. (6.19 – 6.21).

However, the measure contributes differently to the multiverse force. It does not contribute to the force on ρ_Λ , but instead favors late times of observation, $t_{\text{vir}} + t_{\text{obs}}$,

because the mass inside the causal diamond depends linearly on this quantity as long as it does not exceed t_Λ . This corresponds to a contribution of a force of strength 1 on the variable $t_{\text{vir}} + t_{\text{obs}}$:

$$\Delta p_{\text{vir+obs}} = 1. \quad (6.25)$$

In terms of the individual variables, t_{vir} and t_{obs} , this implies that for $t_{\text{vir}} \gg t_{\text{obs}}$, the CD measure contributes $(\Delta p_{\bar{\rho}}, \Delta p_\Lambda, \Delta p_{\text{obs}})_{\text{CD}} = (-\frac{1}{2}, 0, 0)$; in the opposite limit, $(0, 0, 1)$.

Thus, the force is not uniform in the allowed quadrant of parameter space; instead, it changes across the hypersurface $t_{\text{vir}} \sim t_{\text{obs}}$. This case cannot be treated with the simple analysis following Eq. (2.8), and we will not attempt here to constrain the prior force strengths and directions compatible with the observed values of the three parameters.

We note, instead, that the measure force $\Delta p_{\text{vir+obs}}$ acts to increase $t_{\text{vir}} + t_{\text{obs}}$. Because of the constraint Eq. (6.1) that arises in this measure, it also acts to increase t_Λ with strength 1, or equivalently to decrease Λ with strength $-1/2$. Therefore, the measure force effectively counteracts the prior pressure towards large Λ , reducing it from 1 to $1/2$. This is similar to the causal patch, where this reduction happens more directly, without the need to invoke one of the catastrophic boundaries; see Eqs. (6.23, 6.24). We thus expect that the causal diamond, like the patch, leads to a good agreement between observed and predicted values for these three parameters, for a reasonable range of prior force strengths $(p_{\bar{\rho}}, p_{\text{obs}})$.

6.5 Forces with the modified scale factor measure

Finally, let us turn to SF2, a version of the scale factor measure that requires $t_{\text{vir}} + t_{\text{obs}} < t_\Lambda$ [9]. We may again translate this condition into the two boundaries given in Eqs. (5.1, 6.2).¹⁰ Thus, the catastrophic boundaries are the same as for the other two measures considered in this section. And so the SF2 measure, too, gives rise to the general prediction that we should find ourselves near the triple critical point $(\bar{\rho}_c, \rho_{\Lambda,c}, t_{\text{obs},c})$, and to the empirical constraints given in Eqs. (6.19 – 6.21).

However, the SF2 measure makes contributions to the forces that differ strongly from those arising from the CP or CD. It weights by the physical density of observers, which is proportional to $(t_{\text{vir}} + t_{\text{obs}})^{-2}$. Thus, for $t_{\text{vir}} \gg t_{\text{obs}}$, it contributes

¹⁰Strictly, the SF2 measure involves an effective t_{obs} related to the time when the latest geodesic reaching observers achieved maximum expansion. One would expect that this occurs at about one half of the time $t_{\text{vir}} + t_{\text{obs}}$, so one should redefine $t_{\text{obs,SF2}} = (t_{\text{obs,CP}} - t_{\text{vir}})/2$. However, compared to the CP, the SF2 measure suppresses large values of $\rho_\Lambda \gtrsim t_{\text{obs}}^{-2}/G_N$ by an additional factor $\rho_\Lambda^{-3/2}$; so the sharp boundary on t_{obs} , which was $t_{\text{obs,CP}} < t_\Lambda$, should also be moved to a smaller value. If we choose $t_{\text{obs,SF2}} < t_\Lambda/2$, then these two effects roughly cancel, so we will omit both from our analysis for simplicity.

$(\Delta p_{\bar{\rho}}, \Delta p_{\Lambda}, \Delta p_{\text{obs}})_{\text{SF2}} = (1, 0, 0)$; in the opposite limit, $(0, 0, -2)$. This is unhelpful, because both contributions go in the wrong direction: by Eq. (6.21), p_{obs} must be positive, and by Eqs. (6.19, 6.20), $p_{\bar{\rho}}$ must be negative. Thus, the empirical constraints require that large landscape forces $\tilde{p}_{\bar{\rho}} < 0$ and $\tilde{p}_{\text{obs}} > 0$ overcompensate for the contribution from the measure. This is particularly acute for p_{obs} , which must be larger than in the CP measure by about 1, in order to compensate for the larger value of p_{Λ} (1 instead of $1/2$) in Eq. (6.20). But we cannot exclude the SF2 measure; it is possible that the prior distributions in the landscape satisfy these constraints.

7. Predicting the Primordial Density Contrast

Our halo, which is among the largest galactic halos, virialized approximately 3 Gyr after the big bang. According to Eq. (3.21), Compton cooling in our universe became ineffective only a little earlier, at 360 million years. We have argued that there is an environmental understanding of why the Milky Way halo was just able to cool radiatively, could it be that there is also an environmental reason to explain why it just failed to cool by inverse Compton scattering?

Indeed, the proximity to Compton cooling is striking. For example, with Q a factor of 4 larger than in our universe (and holding fixed the temperature at equality), a halo with the mass of the Milky Way would have undergone Compton cooling. This suggests that there is a catastrophic boundary associated with Compton cooling, and that the multiverse distribution has pushed us close to it. In this section, we will explore the consequences of such a boundary. We stress that we do not explain why the anthropic weighting factor varies suddenly across the Compton boundary; we will simply pursue the consequences of *assuming* that it does.

7.1 Catastrophic boundary from Compton cooling

As discussed in section 3.4, Compton cooling is effective if $t_{\text{comp}} < t_{\text{vir}}$; this is the case for all galaxies that form prior to the cosmological time $t_{\text{comp,max}}$ given in Eq. (3.21). We are assuming that Compton cooling inhibits the formation of galaxies, or changes their structure sufficiently to make them inhabitable. In our universe, Compton cooling only affects halos that virialize very early and thus have small mass. We have defined a catastrophe as the absence of habitable galaxies of any mass scale. Thus, a catastrophe occurs if parameters are altered so that Compton cooling affects *all* halos, including those of the largest mass able to cool radiatively, M_+ , given in Eq. (3.14). Namely, a catastrophe is averted if

$$t_{\text{comp,max}} < t_{\text{vir}}(M_+). \quad (7.1)$$

Using Eq. (3.4), we thus find the catastrophic boundary

$$Q^2 \bar{\rho} < \frac{3^6 \times 5 N_{\text{eq}} c_{\text{vir}}^{10/3} \delta_{\text{col}}^5}{2^{10} \pi^{1/3} f(M_+)^5} \frac{G_N m_e^6}{\alpha^4}. \quad (7.2)$$

We could have expressed this boundary in terms of any two of the three parameters Q , T_{eq} , and $\bar{\rho} = Q^3 T_{\text{eq}}^4$. For continuity with the previous sections, we have chosen to retain $\bar{\rho}$ as a scanning parameter.

There is a subtlety here. Compton cooling can be catastrophic only if it is faster than radiative cooling; otherwise, it would have no opportunity to act. However, this condition will automatically be satisfied if the above inequality is violated. For the largest halos able to cool radiatively, $t_{\text{rad}} = t_{\text{vir}}$ by definition, so a violation of Eq. (7.1) implies that Compton cooling is faster than radiative cooling. For smaller halos, which virialize earlier, $t_{\text{comp}} \propto t_{\text{vir}}^{8/3}$ whereas $t_{\text{rad}} \propto t_{\text{vir}}^{5/3}$. Therefore, Compton cooling will be faster than radiative cooling for all halos capable of cooling if Eq. (7.1) is violated.

7.2 Predictions

We can now consider the four-dimensional parameter space $(\bar{\rho}, \rho_{\Lambda}, t_{\text{obs}}, Q)$. We have established four catastrophic boundaries, which intersect at the critical point

$$(\bar{\rho}_c, \rho_{\Lambda,c}, t_{\text{obs},c}, Q_c). \quad (7.3)$$

The first three critical values have been derived in the three previous sections; the fourth can be obtained by setting $\bar{\rho} \rightarrow \bar{\rho}_c$ in Eq. (7.2). Using Eq. (4.1), we find

$$Q_c = \frac{\pi^{1/3} c_{\text{vir}} \delta_{\text{col}} N_{\text{eq}} f_{\rho} K f_B}{8 f(M_c) c_{\text{ion}}^{1/2} f_{\text{rad}}} \frac{m_e}{m_p} \simeq 2.4 \times 10^{-3}. \quad (7.4)$$

As usual, let us now assume that the four-dimensional multiverse force is directed towards the critical point. (We will analyze this condition in detail in the next subsection.) Then we predict

$$Q \sim Q_c, \quad (7.5)$$

in addition to the three other predictions $(\bar{\rho}, \rho_{\Lambda}, t_{\text{obs}}) \sim (\bar{\rho}_c, \rho_{\Lambda,c}, t_{\text{obs},c})$ established in the previous sections. The observed value is $Q_o \simeq 2.0 \times 10^{-5}$, a factor of 120 below the critical value. As a corollary, we are now able to explain the quadruple coincidence

$$t_{\text{comp,max}} \sim t_{\text{obs}} \sim t_{\Lambda} \sim t_{\text{rad}} \sim t_{\text{vir}} \sim \frac{\alpha^2}{G_N m_e^2 m_p} \quad (7.6)$$

of timescales observed in our universe.

7.3 Forces

In addition to the variables z_1, z_2, z_3 defined in section 6.3, we now have the fourth scanning parameter

$$z_4 = \ln \frac{Q}{Q_c}. \quad (7.7)$$

The matrix

$$B = \begin{pmatrix} 1 & 0 & 0 & 0 \\ 1 & -1 & 0 & 0 \\ 0 & -1 & -2 & 0 \\ -1 & 0 & 0 & -2 \end{pmatrix} \quad (7.8)$$

defines the boundary-orthogonal parameter

$$u_4 = \ln \frac{Q_c^2 \bar{\rho}_c}{Q^2 \bar{\rho}}, \quad (7.9)$$

and leaves the definitions of u_1, u_2, u_3 unchanged compared to section 6.3.

By Eq. (2.9), $(B^{-1})^T$ defines a boundary-orthogonal force vector S , with

$$s_1 = p_{\bar{\rho}} + p_{\Lambda} - \frac{1}{2} p_{\text{obs}} - \frac{1}{2} p_Q, \quad (7.10)$$

$$s_2 = -p_{\Lambda} + \frac{1}{2} p_{\text{obs}}, \quad (7.11)$$

$$s_3 = -\frac{1}{2} p_{\text{obs}}, \quad (7.12)$$

$$s_4 = -\frac{1}{2} p_Q. \quad (7.13)$$

The absence of a runaway problem, i.e., the condition that the multiverse force points towards the critical point, is that all $s_i < 0$. In particular, we must assume a statistical preference for large values of Q , which seems entirely natural.

From the observed values in our universe we find

$$u_{1,o} \simeq \ln 40 \simeq 3.7, \quad (7.14)$$

$$u_{2,o} \simeq \ln 139 \simeq 4.9, \quad (7.15)$$

$$u_{3,o} \simeq \ln 2.5 \simeq 0.92, \quad (7.16)$$

$$u_{4,o} \simeq \ln 355 \simeq 5.9. \quad (7.17)$$

By demanding that these observed values are within one or two standard deviations from the median, we obtain from Eq. (2.13) that

$$p_{\bar{\rho}} + p_{\Lambda} - \frac{1}{2} p_{\text{obs}} - \frac{1}{2} p_Q = - \left[0.19 \begin{smallmatrix} +0.31 \\ -0.14 \end{smallmatrix} (1\sigma) \begin{smallmatrix} +0.84 \\ -0.18 \end{smallmatrix} (2\sigma) \right], \quad (7.18)$$

$$-p_{\Lambda} + \frac{1}{2} p_{\text{obs}} = - \left[0.141 \begin{smallmatrix} +0.233 \\ -0.106 \end{smallmatrix} (1\sigma) \begin{smallmatrix} +0.626 \\ -0.136 \end{smallmatrix} (2\sigma) \right], \quad (7.19)$$

$$-\frac{1}{2} p_{\text{obs}} = - \left[0.76 \begin{smallmatrix} +1.25 \\ -0.57 \end{smallmatrix} (1\sigma) \begin{smallmatrix} +3.37 \\ -0.73 \end{smallmatrix} (2\sigma) \right], \quad (7.20)$$

$$-\frac{1}{2} p_Q = - \left[0.12 \begin{smallmatrix} +0.20 \\ -0.09 \end{smallmatrix} (1\sigma) \begin{smallmatrix} +0.53 \\ -0.11 \end{smallmatrix} (2\sigma) \right]. \quad (7.21)$$

The first three constraints are identical to those found in section 6.3, except that the contribution to the multiverse force from p_Q is now made explicit on the left hand side.

How do these bounds compare to theoretical expectations? We will discuss only the causal patch measure here, which leads to the force $p_{\Lambda} = \frac{1}{2}$ on the cosmological constant. With this value, the above constraints can easily be satisfied at the 1σ level with natural force strengths, e.g., with $(p_{\bar{\rho}}, p_{\text{obs}}, p_Q) = (-\frac{1}{2}, \frac{1}{2}, \frac{1}{2})$, $(-\frac{1}{4}, \frac{1}{2}, \frac{1}{4})$ or $(-\frac{1}{4}, \frac{3}{4}, \frac{1}{2})$.

8. Discussion

We have found that multiverse forces and catastrophic boundaries can explain the quadruple coincidence of timescales, Eq. (1.1), or equivalently, the observed values of the virial density, the cosmological constant, the observer timescale, and the timescales for radiative and Compton cooling.

As more parameters are taken to scan, dare we think that all fundamental parameters could be determined in this way? The answer is clearly no: as far as we know many parameters, such as the strong CP parameter and the τ lepton mass, are not relevant for any catastrophic boundary. Still, could it be that all the parameters that do enter catastrophic boundaries get determined environmentally? For the boundaries considered so far, the relevant set of parameters is

$$\alpha, m_e, m_p, G_N, Q, T_{\text{eq}}, \rho_{\Lambda}, \eta_B, \quad (8.1)$$

where η_B is the number density of baryons relative to photons. Depending on the measure used to compute the statistical averages we could also include t_{obs} . If all the parameters of Eq. (8.1) scan independently then the structure and cooling boundaries can determine ρ_{Λ} , Q , T_{eq} (and t_{obs}), but what of the others?

The ratio m_e/m_p plays an important role in the boundaries of nuclear stability, leaving α, m_p, η_B and G_N . The proton mass is directly derived from the QCD scale,

Λ_{QCD} , and we can assume that this is related to α by gauge coupling unification¹¹ — i.e. we are not quite right to say that all the parameters of Eq. (8.1) scan independently. Taking G_{N} to set the unit of energy, M_{Pl} , leaves just two undetermined dimensionless parameters: η_B and $\Lambda_{\text{QCD}}/M_{\text{Pl}}$. Thus the landscape force and catastrophic boundaries have rigidly determined the entire parameter set of Eq. (8.1), with the exception of the baryon asymmetry and an overall mass hierarchy. In fact, they may overdetermine it if t_{obs} is a function of the parameters listed in Eq. (8.1). This, however, is not the case if t_{obs} is very sensitive to the values of α, m_e, \dots , so that it can take a wide range of values within the parameter space in which the fundamental parameters, α, m_e, \dots , satisfy the nuclear stability and other requirements. In such a case, t_{obs} can be viewed as an independent scanning parameter.

Our universe lies at the tip of a cone in the four dimensional parameter space of $\{m_e/m_p, Q, T_{\text{eq}}, \rho_\Lambda\}$ (or of five dimensional space including t_{obs}); but when an additional dimension such as η_B and $\Lambda_{\text{QCD}}/M_{\text{Pl}}$ is added, a runaway behavior could reemerge. It is, however, possible that the direction opened by the addition of a new parameter is again constrained by a new catastrophic boundary containing that parameter. For example, the up and down quark masses are constrained by further nuclear stability boundaries, and the weak scale and baryon asymmetry play a crucial role at the boundary associated with big bang nucleosynthesis. Given these possible boundaries, we can imagine that most of the environmentally relevant parameters in the standard particle physics and astrophysics are determined by multiverse physics as described here.

Ultimately, an important question will be what determines the overall mass hierarchy between the Planck and particle physics mass scales, allowing the existence of large observable universe. We see three different possibilities:

- The multiverse distribution function. For example, the unified coupling at the Planck scale may have a distribution $f(\alpha)$ peaked around some perturbative value that corresponds to a peak in the distribution for Λ_{QCD} exponentially below M_{Pl} .
- A further catastrophic boundary. As $\Lambda_{\text{QCD}}/M_{\text{Pl}}$ grows, complex structures such as the sun will get smaller, and eventually cause catastrophic changes. Perhaps our universe is already close to some such boundary. In this case, n catastrophic boundaries constrain n scanning parameters. (Throughout this paper we have assumed a multiverse force that places typical observers in universes near the tip of a cone. An alternative possibility is that the observer region in the n dimensional space is very small.)

¹¹The relation involves the weak scale, which may be determined by some other boundary.

- The discretuum. The vacuum energy scales as the 6th power of the overall hierarchy: $\rho_\Lambda \propto (\Lambda_{\text{QCD}}/M_{\text{Pl}})^6$, given that environmental selection by nuclear stability sets $m_e \sim m_p \sim \Lambda_{\text{QCD}}$. Suppose that $f(\alpha)$ gives a force to low values of $(\Lambda_{\text{QCD}}/M_{\text{Pl}})$. The vacuum energy may become so small that the discreteness of the string landscape will become apparent, eventually stopping the potential runaway. If this is the origin of the overall hierarchy, the number of string vacua is of order $M_{\text{Pl}}^4/\rho_\Lambda \approx 10^{120}$.

At present we are unable to compute the overall hierarchy, no matter how it is determined. Nevertheless, we are encouraged that simple arguments based on galaxy cooling allow a broad numerical understanding of ρ_Λ , M_{gal} , Q and T_{eq} in terms of the fundamental parameters in particle physics, α , m_e , m_p and G_{N} .

Acknowledgments

We thank Roni Harnik, Stefan Leichenauer and Jens Niemeyer for discussions. This work was supported in part by the Director, Office of Science, Office of High Energy and Nuclear Physics, of the US Department of Energy under Contract DE-AC02-05CH11231, and in part by the National Science Foundation under grant PHY-0457315. The work of R.B. was supported in part by a Career grant of the National Science Foundation. The work of Y.N. was supported in part by the National Science Foundation under grant PHY-0555661 and by the Alfred P. Sloan Foundation.

References

- [1] F. J. Dyson, *Rev. Mod. Phys.* **51**, 447 (1979).
- [2] S. Weinberg, *Phys. Rev. Lett.* **59**, 2607 (1987).
- [3] J. D. Barrow and F. J. Tipler, *The Anthropic Cosmological Principle* (Oxford University Press, Oxford, United Kingdom, 1986).
- [4] G. Efstathiou, *Mon. Not. Roy. Astron. Soc.* **274**, L73 (1995); H. Martel, P. R. Shapiro and S. Weinberg, *Astrophys. J.* **492**, 29 (1998) [arXiv:astro-ph/9701099]; J. Garriga, M. Livio and A. Vilenkin, *Phys. Rev. D* **61**, 023503 (2000) [arXiv:astro-ph/9906210].
- [5] R. Bousso, *Phys. Rev. Lett.* **97**, 191302 (2006) [arXiv:hep-th/0605263].
- [6] R. Bousso, R. Harnik, G. D. Kribs and G. Perez, *Phys. Rev. D* **76**, 043513 (2007) [arXiv:hep-th/0702115].
- [7] L. J. Hall and Y. Nomura, *Phys. Rev. D* **78**, 035001 (2008) [arXiv:0712.2454 [hep-ph]].

- [8] A. De Simone, A. H. Guth, M. P. Salem and A. Vilenkin, arXiv:0805.2173 [hep-th].
- [9] R. Bousso, B. Freivogel and I. S. Yang, arXiv:0808.3770 [hep-th].
- [10] R. Bousso and J. Polchinski, JHEP **0006**, 006 (2000) [arXiv:hep-th/0004134]; S. Kachru, R. Kallosh, A. Linde and S. P. Trivedi, Phys. Rev. D **68**, 046005 (2003) [arXiv:hep-th/0301240]; L. Susskind, arXiv:hep-th/0302219; M. R. Douglas, JHEP **0305**, 046 (2003) [arXiv:hep-th/0303194].
- [11] M. Tegmark, A. Aguirre, M. J. Rees and F. Wilczek, Phys. Rev. D **73**, 023505 (2006) [arXiv:astro-ph/0511774].
- [12] M. J. Rees and J. P. Ostriker, Mon. Not. R. astr. Soc. **179**, 541 (1977).
- [13] J. Silk, Astrophys. J. **211**, 638 (1977).
- [14] S. D. M. White and M. J. Rees, Mon. Not. R. astr. Soc. **183**, 341 (1978).
- [15] M. Tegmark and M. J. Rees, Astrophys. J. **499**, 526 (1998) [arXiv:astro-ph/9709058].
- [16] B. J. Carr and M. J. Rees, Nature **278**, 605 (1979).
- [17] D. N. Page, arXiv:hep-th/0610079.
- [18] R. Bousso and B. Freivogel, JHEP **0706**, 018 (2007) [arXiv:hep-th/0610132].
- [19] R. Bousso, B. Freivogel and I. S. Yang, Phys. Rev. D **77**, 103514 (2008) [arXiv:0712.3324 [hep-th]].